Atomic pair production by photons in the threshold region

J. Basu, S. K. Sen Gupta, N. C. Paul, S. C. Das, and N. Chaudhuri
Department of Physics, North Bengal University, Pin 734430 Darjeeling, India
(Received 18 August 1980)

New results of relatively high-precision measurements to study atomic pair production by photons in the threshold region together with some other previous measurements are presented for a critical evaluation of the new calculations with corrections of Coulomb effect and atomic-electron screening effect in the low-energy pair production. This evaluation reveals the degree in which the theory is in greater agreement with measurements in the threshold region and indicates the trend of cross sections as a function of atomic number and photon energy.

I. INTRODUCTION

A significant advance has been made in recent years in the theoretical calculations of atomic pair production by photons, photoionization of atoms, and atomic coherent and incoherent scattering of photons. The accuracy of cross sections from these calculations has greatly increased compared to the accuracy of earlier calculations which have been employed in the analysis of previous measurements of total and partial cross sections. Several of the "direct" measurements of the partial cross sections of the atomic pair-production process are subject to considerable inherent difficulties and uncertainty arising from poor statistics and consequently show wide variations in the data. A few of the experiments in which agreement was found with old calculations should be reanalyzed in view of the latest theoretical work of much reduced uncertainty. Measurements of total cross sections from attenuation of photon beams in high-Z elements lead to determination with relatively higher precision of the pair-production cross section through the use of very accurate atomic cross sections of the competing processes. Since it has been difficult so far to avoid systematic errors and improve statistics in the low-energy direct pair-production measurements, high-precision total cross-section experiments appear to deserve further attention. In this paper we attempt a study of atomic pair production in the threshold region (1.02–5 MeV) through an evaluation of some of the more recent measurements representing considerable improvements in precision over earlier measurements and our own attenuation measurements at four-photon energies (1.115, 1.119, 1.173, and 1.332 MeV) on eight elements in the range Z = 42–82. The aim of this study is to indicate the degree to which the measurements show unity in the data and with the currently available refined theoretical cross sections of the atomic pair-production process.

II. PRESENT MEASUREMENTS

The attenuation of a photon beam has been measured very carefully to obtain total cross sections for eight elements in the range Z = 42–82 at four-photon energies in the pair-production-threshold region. A schematic diagram of the experimental arrangement is shown in Fig. 1. Transmission of an extremely narrow collimated beam of photons through 2–3 mean-free-path lengths of absorber and a high degree of collimation of the beam after transmission through the absorber excluded multiple scattering effects in the absorber and prevented the photons scattered in the absorber at scattering angles greater than 20′–24′, from reaching the detector. Within such a geometry the effect of scattering at angles smaller than 24′ was so small it gave a systematic error which was much less than the statistical error of 0.3% in the measurements.

With the use of a 10-cm^2 cylindrical NaI(Tl) scintillator head, the spectra of the primary and transmitted photons through the absorber were recorded in the same counting channels of the analyzer to eliminate photons scattered from objects other than the absorber sample. The details of counting are the same as given in a previous paper.[1]

III. EXPERIMENTAL DATA AND ERRORS

For the purpose of the present analysis, we have included for evaluation some additional results from the following recent measurements: (a) Total attenuation measurements of (i) Henry and Kennett[2] at ten different energies (from 1.778 to 4.508 MeV) on four elements (Z = 29, 42, 82, and 92), (ii) Conner *et al.*[3] at three photon energies (1.115, 1.598, and 2.754 MeV) on four elements (Z = 29, 42, 82, and 92), and (iii) Colgate[17] at two photon energies (1.332 and 2.62 MeV) on lead (Z = 82); (b) Direct measurements of (i) Avignone *et al.*[4] at 1.332 and 2.615 MeV on Z

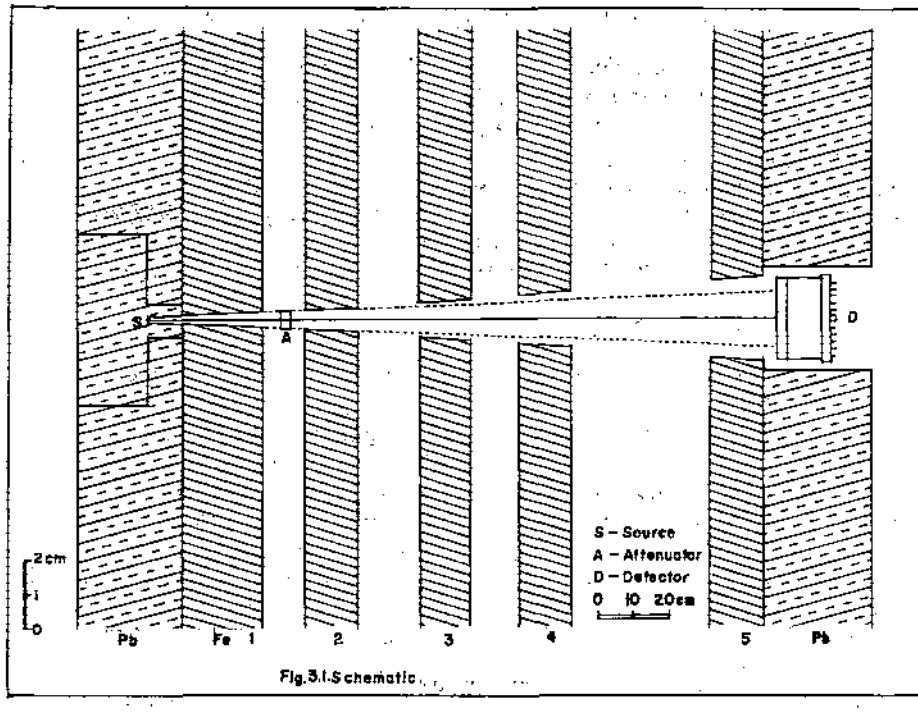

FIG. 1. Schematic diagram of the experimental arrangement.

= 50, (ii) Henry and Kennett[5] at three photon energies (1.173, 1.332, and 2.754 MeV) on four elements ($Z = 29$, 42, 53, and 82), (iii) T. A. Girard *et al.*[6] at 1.119 and 2.615 MeV on four elements ($Z = 13$, 29, 50, and 82); (iv) J. Rama Reo *et al.*[7] at 1.119 MeV on eight elements ($Z = 29$ to 82) and (v) Dayton[8] at 1.332 and 2.615 MeV on four elements ($Z = 29$, 50, 82, and 92). Some of the measurements in these two classes overlap both in photon energy and target element and thus help obtain a consistency check in the analysis.

The errors to our measured total cross sections arising out of statistical uncertainty was in the range 0.1–0.3%. In addition to statistical uncertainty, the systematic errors arising from geometry, target, source size, and background scattering effects have been reduced to an extent less than the statistical error. The correction due to experimental limitation of complete discrimination when a gamma-ray source emits photons of more than one energy has been applied to the data.

IV. COMPUTATION OF THEORETICAL CROSS SECTIONS

In the threshold region (1.02–5 MeV) the atomic pair-production cross sections have been computed from the latest calculations for pair production in the nuclear Coulomb field by Tseng and Pratt,[9] Øverbø *et al.*,[10] and Øverbø.[11] These treatments include atomic electron screening and Coulomb effects, but the calculation of Øverbø *et al.*[10] and Øverbø[11] is valid only above a photon energy of 1.25 MeV for high-Z atoms. Above a photon energy of 2 MeV we have also included the cross sections for triplet production according to the calculations as summarized by Hubbell.[12]

For the present purpose it was also necessary to compute the contributions of other competing interaction processes: atomic photoionization, and incoherent and coherent scattering of photons. The cross sections of these three processes are now known theoretically to a high degree of accuracy and we have computed these using the following calculations: (i) Theoretical atomic photoionization cross sections in the range 1.0–1.5 MeV from Scofield[13] in 1.5–3 MeV from Schmickley and Pratt,[14] and in 3–5 MeV from the compilation of Hubbell.[12] (ii) Hartree-Fock atomic incoherent and coherent scattering factors of Crommer and Mann[15] as compiled by Hubbell *et al.*[16]

V. DISCUSSION OF RESULTS

The main point to be made is presented in Figs. 2–4 where total cross-section results from attenuation measurements are displayed together with theoretical curves for the combined interaction processes involved. Theoretical curves of var-

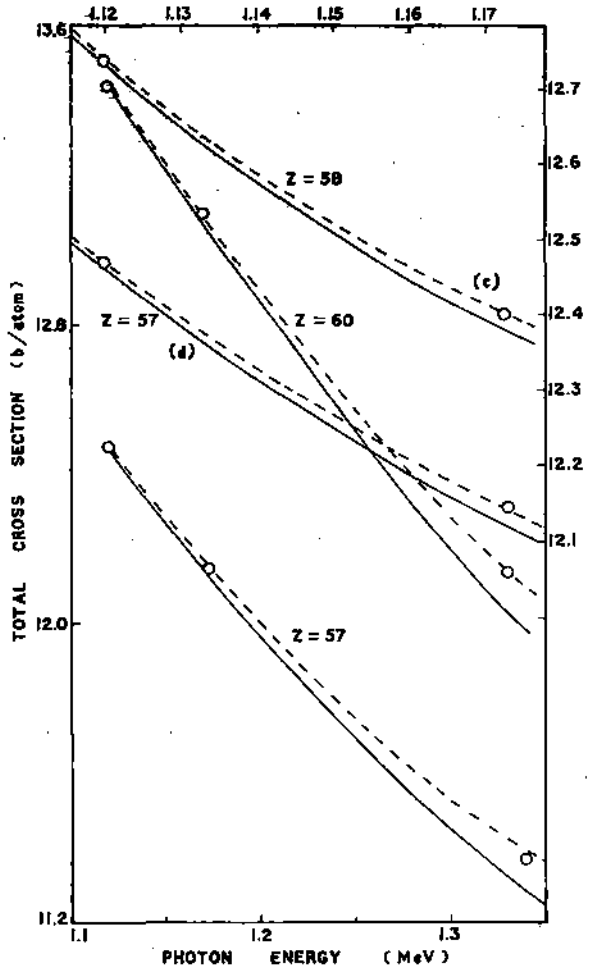

FIG. 2. Total cross section versus photon energy. – – – – – – theoretical total cross section and ——— total cross section less the Tseng-Pratt (Ref. 9) pair-production cross section. The experimental points are for $Z = 57$, 58, and 60. Top and right-hand scales are for curves (c) and (d).

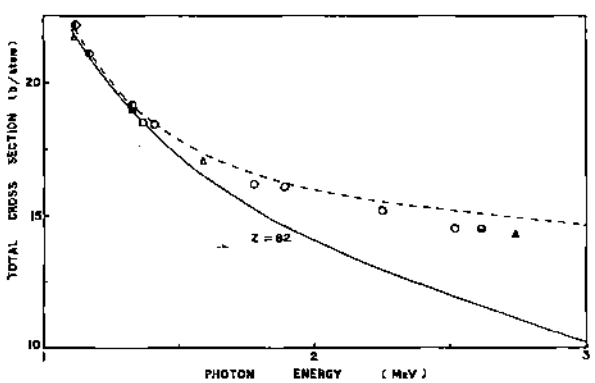

FIG. 3. Same as in Fig. 2 but for Pb. Experimental points: ⊙—our experiments, ○—Henry and Kennett (Ref. 2), △—Conner *et al.* (Ref. 3), and ◐—Colgate (Ref. 17).

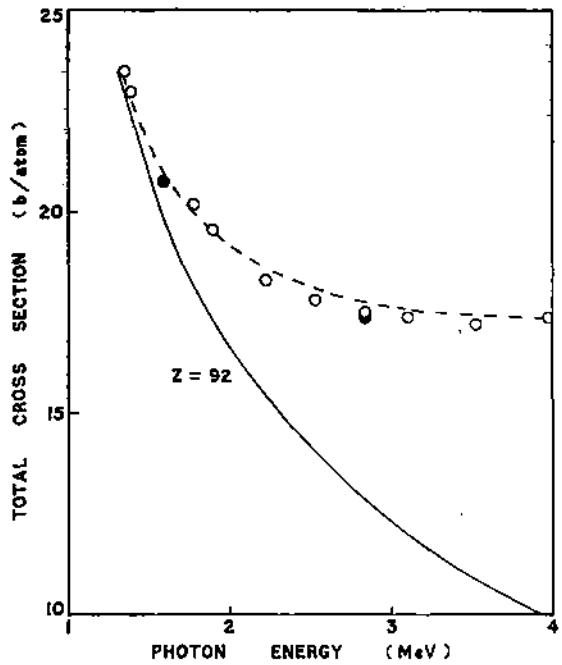

FIG. 4. Same as in Fig. 2 but for U. Experimental points: ●—Conner *et al.* (Ref. 3) and ○—Henry and Kennett (Ref. 2).

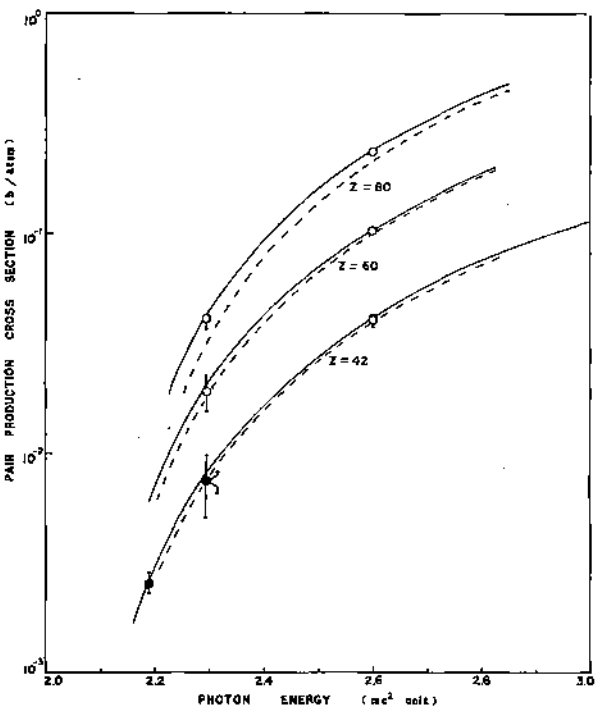

FIG. 5. Pair-production cross section versus photon energy for $Z = 42$, 60, and 80. Curve – – – – – – Øverbø *et al.* (Ref. 10), curve ——— Tseng-Pratt (Ref. 9), ○—our experiments, and ●—Henry and Kennett (Ref. 5).

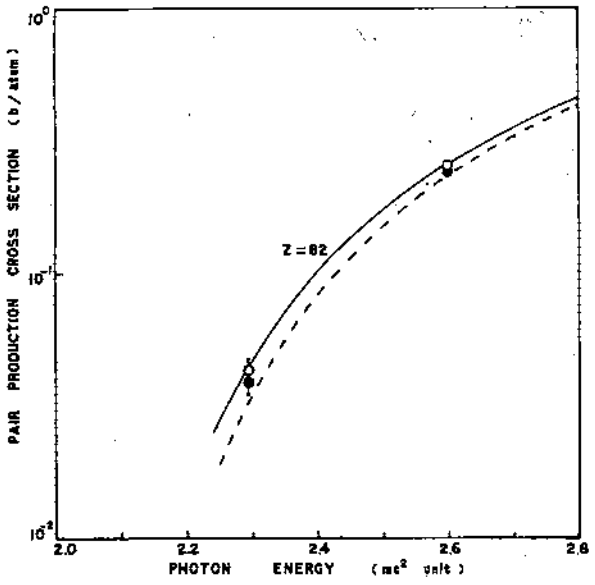

FIG. 6. Same as in Fig. 5, but for Pb. ○—our experiments and ●—Henry and Kennett (Ref. 5).

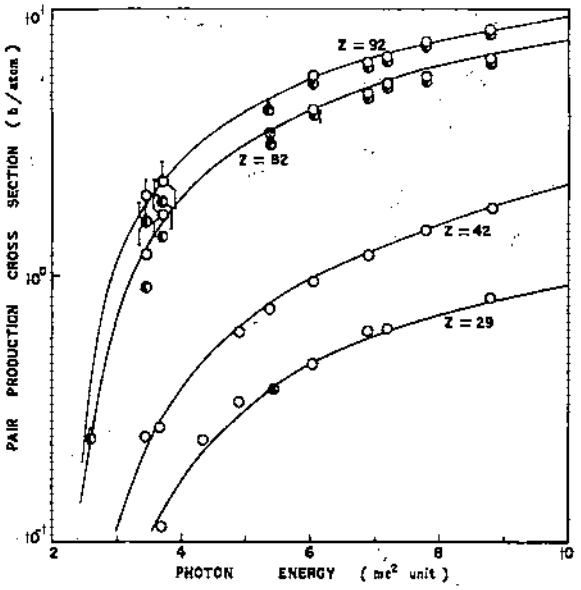

FIG. 7. Same as in Fig. 5 but for $Z = 29$, 42, 82, and 92. Theoretical curves: ——— Tseng-Pratt (Ref. 9), ○—our reanalysis of total cross-section data of Henry and Kennett (Ref. 2), ▲—our reanalysis of total cross-section data of Conner *et al.* (Ref. 3), ●—Henry and Kennett (Ref. 2), and △—our experiments.

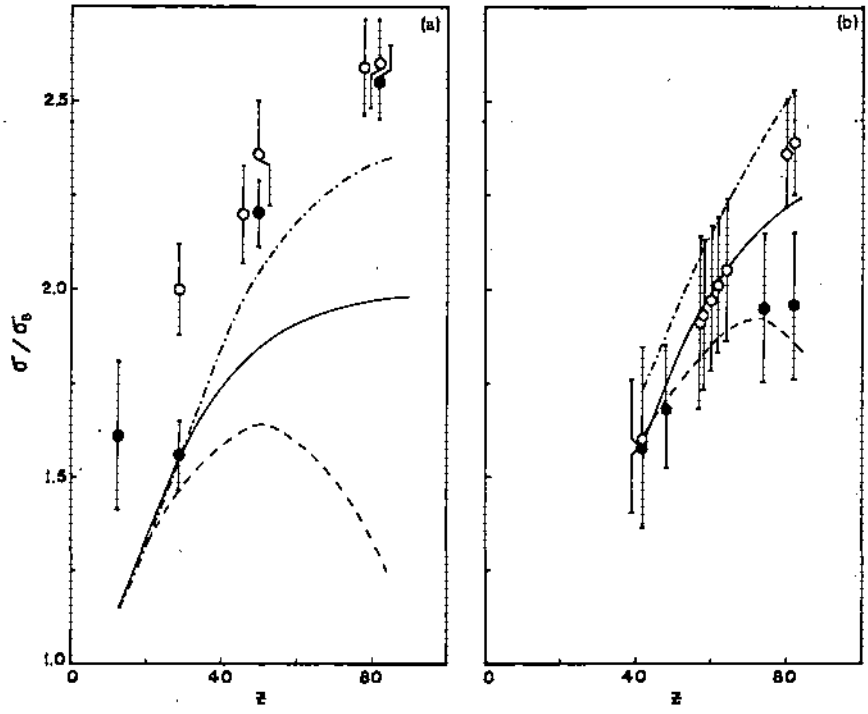

FIG. 8. σ/σ_B versus Z. For 1.119 MeV (a) and for 1.173 MeV(b): curve – – – – Øverbø *et al.*, curve —— Tseng-Pratt (Ref. 9), and curve - · - · - Øverbø (Ref. 11). Experimental points for 1.119 MeV: ○—Girard *et al.* (Ref. 6) and ●—Rao *et al.* (Ref. 7), for 1.173 MeV: ○—our experiments and ●—Henry and Kennett (Ref. 5).

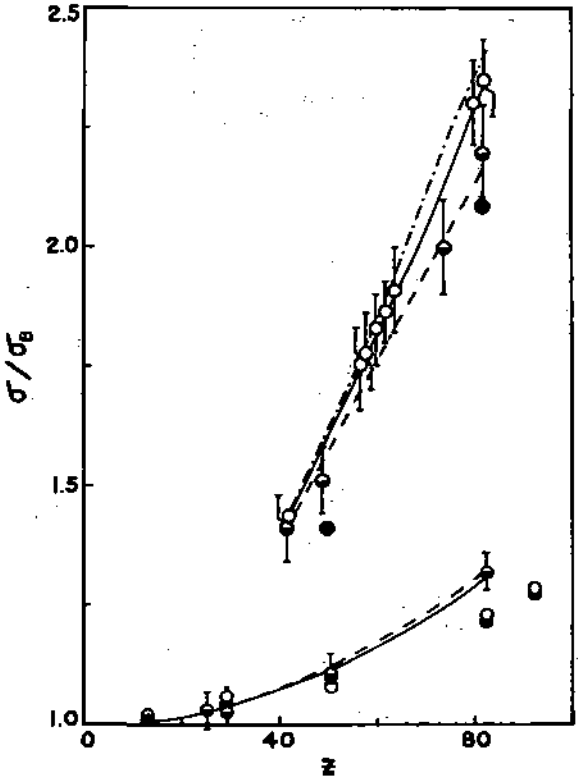

FIG. 9. Same as in Fig. 8. Upper: 1.332 MeV, curve – – – – – – Øverbø *et al.* (Ref. 10), curve —— Tseng-Pratt (Ref. 9), and curve – · – · – Øverbø (Ref. 11). Experimental points: ○—our experiments, ▪—Henry and Kennett (Ref. 5), and ●—Dayton (Ref. 8). Lower: 2.615 MeV, curve – – – – Tseng-Pratt (Ref. 9), curve —— Øverbø *et al.* Experimental points: ⊖—Girard *et al.* (Ref. 6), ○—Dayton (Ref. 8), and ●—our reanalysis of Colgate's data.

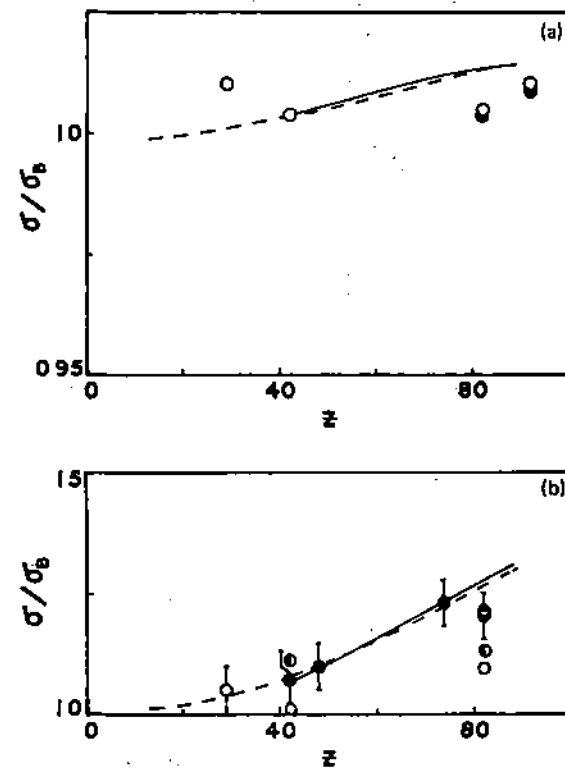

FIG. 10. Same as in Fig. 8. (a) for 3.53 MeV: curve – – – – – Øverbø *et al.* (Ref. 10) and curve —— Tseng-Pratt (Ref. 9). Experimental points: ●—Henry and Kennett (Ref. 2) and ○—our reanalysis of Henry and Kennett's data. (b) for 2.754 MeV: curve – – – Øverbø *et al.* (Ref. 10) and curve —— Tseng-Pratt (Ref. 9). Experimental points: ●—Henry and Kennett (Ref. 2), ○—our reanalysis of Henry and Kennett's data, ⊖—our reanalysis of the data of Conner *et al.*, and ⊖—Standil and Shkolnik (Ref. 19).

ious processes are shown as a function of photon energy in two ways: (a) combined contributions of atomic photoionization and incoherent and coherent scattering of photons and (b) atomic pair production, triplet production, photoionization, and coherent and incoherent scattering of photons. Such a presentation has been given for four elements ($Z = 57$, 60, 82, and 92).

It is seen that this method is adequately suited for inferring an unambiguous conclusion on pair-production theory in the threshold region.

In Figs. 5–7 we have the results of present measurements, the reanalyzed results of some of the previous measurements, and results of some direct measurements displayed together with a combined theoretical atomic pair-production and triplet-production cross sections. The purpose is to demonstrate much larger unity in the data and the theoretical cross sections for the same atom at the same energy.

Figures 8–11 show the dependence relative to the Born approximation result[12] of the theoretical atomic pair-production cross sections on the atomic number at several photon energies in the threshold region. At 1.173 and 1.332 MeV, where direct measurements on the high-Z elements of Henry and Kennett[5] show appreciable differences with calculations of Tseng and Pratt[9] and of Øverbø,[11] the present measurements indicate (i) excellent agreement with the results of Tseng and Pratt[9] in the range of $Z = 42$–82 at 1.332 MeV, (ii) agreement in the medium-Z atoms at 1.173 MeV with Tseng and Pratt,[9] and (iii) a trend in support of the calculation of Øverbø[11] for high-Z elements at 1.173 MeV. In the near-threshold region below 1.173 MeV, where disagreement between direct measurements and the theoretical predictions is greatest (Fig. 8) our measurements indicate unity with theory, although the method is not sensitive enough at these low energies to distinguish

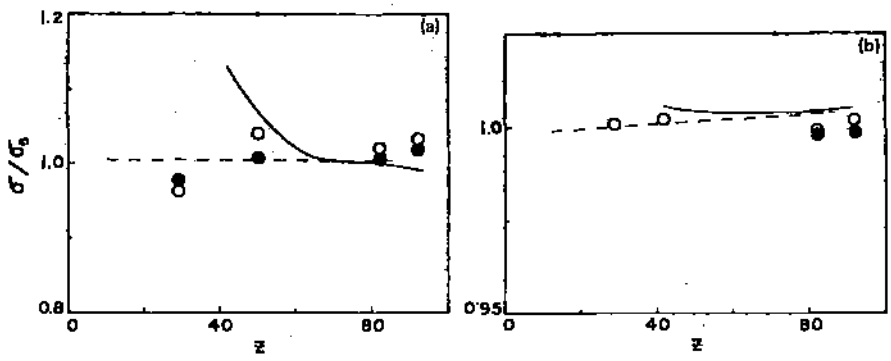

FIG. 11. Same as in Fig. 8. (a) for 5.3 MeV: curve – – – – Øverbø *et al.* (Ref. 10) and curve ——— Tseng-Pratt (Ref. 9). Experimental points: o—Rosenblum *et al.* (Ref. 18) and •—our reanalysis of Rosenblum's data. (b) for 4.50 MeV: curve – – – – Øverbø *et al.* (Ref. 10) and curve ——— Tseng-Pratt (Ref. 9). Experimental points: •—Henry and Kennett (Ref. 2) and o—our reanalysis of the data of Henry and Kennett.

between the results of Øverbø and of Tseng and Pratt. In Fig. 8, the error bars to the data points at 1.119 MeV of Girard *et al.*[6] do not touch the screening-corrected theoretical curve of Øverbø,[11] except the point for $Z = 29$ at which disagreement disappears.

VI. CONCLUSION

In this paper we have attempted only to indicate how very careful total attenuation experiments, in conjunction with very accurate theoretical cross sections for the various competing interaction processes, have provided a check on the recent pair-production theoretical cross section in the threshold region. While it is desirable to perform direct experiments to test the theory at low energies, in practice such experiments have been found to be of limited value in view of inherent difficulties and poor counting statistics. The analysis that has been given shows that the theory of atomic pair production by photons in the threshold energy region appears in greater accord with very accurate total cross-section measurements when corrections for Coulomb and screening effects are included in calculating pair-production cross sections for medium- and high-Z atoms.

ACKNOWLEDGMENTS

The authors wish to thank the University of North Bengal for providing U.G.C. Teacher Fellowships to J. Basu, S. K. Sen Gupta, and N. C. Paul, and a Junior Research Fellowship to S. C. Das, and also the Department of Physics, North Bengal University for providing various facilities to carry out the measurements.

[1]S. K. Sen Gupta, N. C. Paul, S. C. Roy, and N. Choudhuri, J. Phys. B 12, 1211 (1979).
[2]L. C. Henry and T. J. Kennett, Can. J. Phys. 49, 1167 (1971).
[3]A. L. Conner, H. F. Atwater, Elizabeth H. Plassmann, and J. H. McCrary, Phys. Rev. A 1, 539 (1970).
[4]F. T. Avignone III and S. M. Blankenship, Phys. Rev. A 10, 793 (1974).
[5]L. C. Henry and T. J. Kennett, Can. J. Phys. 50, 2756 (1972).
[6]T. A. Girard, F. T. Avignone III, and S. M. Blankenship, Phys. Rev. A 17, 218 (1978).
[7]J. Rama Rao, V. Lakshminarayana, and S. Jnanananda, Proc. Phys. Soc. London 81, 949 (1963).
[8]I. E. Dayton, Phys. Rev. 89, 544 (1953).
[9]H. K. Tseng and R. H. Pratt, Phys. Rev. A 6, 2049 (1972).
[10]I. Øverbø, K. J. Mork, and H. A. Olsen, Phys. Rev. A 8, 668 (1973).
[11]I. Øverbø, Phys. Scr. 19, 299–306 (1979).
[12]J. H. Hubbell, NSRDS-NBS (USA) 29 (1969).
[13]J. H. Scofield, UCRL-51326 Theoretical Photoionization Cross Sections (1973).
[14]R. D. Schmickley and R. H. Pratt, Phys. Rev. 164, 104 (1967).
[15]D. T. Crommer and J. B. Mann, J. Chem. Phys. 47, 1892 (1967); Acta Crystallogr. Sect. A 24, 321 (1968).
[16]J. H. Hubbell, W. J. Veigele, E. A. Briggs, R. T. Brown, and D. T. Crommer, J. Phys. Chem. Ref. Data 4, 471 (1975).
[17]S. A. Colgate, Phys. Rev. 87, 592 (1952).
[18]E. S. Rosenblum, E. F. Schrader, and R. M. Warner, Jr., Phys. Rev. 88, 612 (1952).
[19]S. Standil and V. Shkolnik, Can. J. Phys. 36, 1154 (1958).

PHYSICAL REVIEW A VOLUME 20, NUMBER 3 SEPTEMBER 1979

Atomic Rayleigh scattering of photons in the momentum-transfer range 0–10mc

S. K. Sen Gupta, N. C. Paul, J. Basu, and N. Chaudhuri
Department of Physics, North Bengal University, Pin 734430, India
(Received 24 January 1979)

The new results of measurements of coherent scattering of photons by bound atomic electrons over a momentum transfer q range 0–4mc together with those from other recent measurements with a coverage in the momentum transfer up to 10mc are presented for a critical evaluation of the previous and new calculations on Rayleigh scattering. This evaluation reveals the ranges of applicability of the form-factor formalism in the nonrelativistic and relativistic domain and demonstrates the trend of behavior of the exact theoretical predictions as a function of $q/\alpha Zm$.

I. INTRODUCTION

We have made a series of precision measurements of the coherent scattering of photons over the energy range 0.100–2.0 MeV. In this energy range atomic Rayleigh scattering is the important process predominating over all other elastic scattering processes which combine coherently. Our interest in the study of coherent scattering processes has arisen due to (i) the new developments in the calculations[1–9] of Rayleigh (R) and Delbruck (D) scattering processes which have reduced considerably the prevailing uncertainty in the knowledge of scattering amplitudes, (ii) the differences[10,11] between the sets of experimental cross section data of early γ-ray measurements using the same photon energies and scattering targets, and (iii) the inadequacy[10,11] of the existing experiments in the evaluation of the present state of the theory of nonresonant atomic scattering process.

In this paper we present the results of our measurements and other more recent measurements and calculations in such a way as to bring out the present status of the various theoretical scattering investigations.

II. MEASUREMENTS

Absolute measurements of the differential coherent atomic scattering cross sections were made as a function of photon momentum transfer to the bound atomic electron defined by $q = 2k \sin(\frac{1}{2}\theta)$, where k is the incident photon energy in units of electron rest mass energy and θ is the scattering angle. The experimental apparatus and the method of measurements have been described in detail elsewhere (Sinha *et al.*[12]). Consequently only the essentials relvant to the present measurements are mentioned. γ-ray sources included radioactive isotopes ^{210}Pb (47 keV), ^{241}Am (59.54 keV), ^{141}Ce (145 keV), ^{203}Hg (279.2 keV), ^{137}Cs (662 keV), ^{65}Zn (1.115 MeV), ^{60}Co (1.17 and 1.33 MeV), and ^{124}Sb (2.09 MeV), the source strength being in the range of 3mci for ^{241}Am to 750mci for ^{124}Sb. The differential cross-section measurements were done for 15 elements representing low-, medium-, and high-Z atoms. The pulse-height spectra were accumulated in a ND1100 multichannel analyzer using a storage time of 20–100 ks. In the annular scatterer geometry [Fig. 1(a)], in addition to the scatterer thickness, radii, and source-scatterer distance, three quantities were needed to obtain the total differential cross section, namely, (i) the total number of scattered photons per second, (ii) the total number of photons per second from a similar weak reference source of the same energy and at the same position of the scatterer, and (ii) the background counts per second, all recorded for the same interval of time.

The total number of scattered photons was determined by summing over the pulses under the photopeak of the scattered spectrum. The cross section for the coherently scattered photons was obtained by subtracting the incoherently scattered photons determined by the calculations based on nonrelativistic Hartree-Fock (NRHF) scattering functions (obtained from Hubbell *et al.*[13]).

For the determination of the cross section at larger scattering angles [Fig. 1(b)] we separated the coherent peak from the incoherent peak in the scattered spectrum so that the ratio of the number of coherently scattered photons to that of the incoherently scattered could be found. This ratio, when combined with the calculated incoherent scattering cross section based on NRHF incoherent scattering functions, yielded coherent scattering cross sections. In the large-angle-measurement geometry both the incident and scattered beams were collimated so that for a very small scatterer in the shape of a right-circular cylinder the maximum solid angle between the scatterer and the detector was 5×10^{-2} sr. Corrections due to such a spread of scattering solid angle are

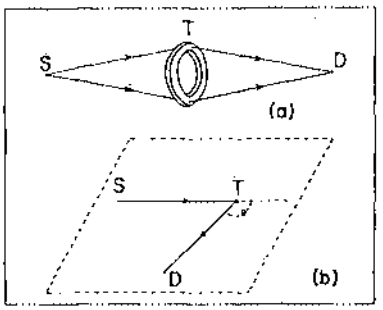

FIG. 1. Schematic diagram of the experimental arrangement (a) for small and (b) for large-angle scattering measurements. *S*, source; *T*, target; and *D*, detector.

generally small, and were taken into account when necessary. The effect of photons suffering multiple scattering in the target and reaching the detector was taken into consideration. In the symmetrical-scattering arrangements (Fig. 1) the photons multiply scattered towards and away from the detector should be mutually compensated to a great extent, therefore, the effect may be neglected since very thin (<3 mm) scatterers were used.

III. EXPERIMENTAL DATA AND ERRORS

For the purpose of the present paper we have presented the cross sections (26 data points in the graph of Fig. 2) of our measurements on Pb ($Z = 82$) for six photon energies: 0.145, 0.280, 0.662, 1.115, 1.17, and 1.33 MeV and we included additional data points for Pb from the following recent high-precision measurements: (i) Schumacher *et al.*,[14] photon energies 59.54 keV (seven data points), 412 keV (eight data points), 662 keV (seven data points), 889 keV (nine data points), 1.12 MeV (nine data points), and 2.75 MeV (eight data points); (ii) Hardie *et al.*,[15] photon energy 1.33 MeV (ten data points); (iii) Kahane *et al.*,[16] photon energy 6.84 MeV (one data point).

The error to the measured cross sections arising from statistical uncertainty was less than 1% in the present and all other measurements listed above. In addition to counting statistics, some sources of systematic errors were considered in the present measurements. Those include uncertainties (i) from the presence of incoherent component in the measurement of coherent component, (ii) in the determination of photopeak area of the coherent component, (iii) variation in the detector background in the presence and absence of of the scatterer, and (iv) in the measurements of source—scatterer distances, scattering angles, thickness of the scatterer, and the photon attenuation coefficient for the scatterer. Some of those errors have been either effectively excluded or minimized and others accounted for with appropriate corrections.

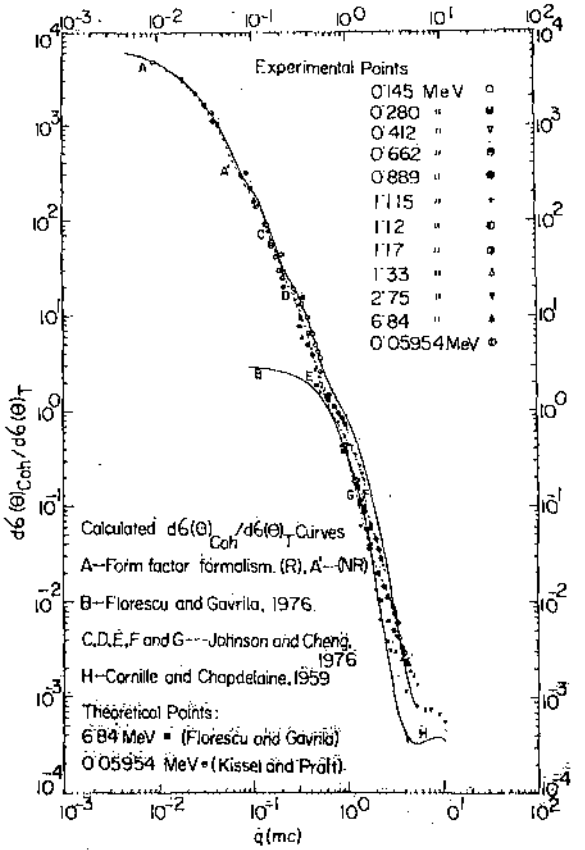

FIG. 2. $d\sigma(\theta)_{coh}/d\sigma(\theta)_T$ plotted vs $q(\hbar c)$.

IV. RAYLEIGH SCATTERING CALCULATIONS

For the interpretation of the data and examining their present status in terms of the theory we have computed theoretical differential cross sections (in units of Thomson cross section per electron) from the following calculations: (i) nonrelativistic Hartree-Fock calculations of the atomic form factor by Cromer and Mann[1] (compiled by Hubbell *et al.*[13]); (ii) relativistic Hartree-Fock (RHF) calculations of the atomic form factor by Doyle and Turner,[2] Cromer and Weber,[3] and ØVerbø[4] (obtained from the compilation of Hubbel *et al.*[5]); (iii) atomic shellwise calculations of the Rayleigh scattering amplitudes by Johnson and Cheng,[6] Cornille and Chapdelaine,[7] and Kissel and Pratt[8]; and (iv) atomic K-shell Rayleigh-scattering amplitude by Florescu and Gavrila.[9]

V. DISCUSSION OF RESULTS AND CONCLUSIONS

The scattering of photons depends on the incident photon energy k, photon scattering angle θ,

and the atomic number Z of the scatterer atom. In order to study the behavior of the coherent scattering cross section as a function of photon momentum transfer q over the energy region where the Rayleigh scattering is predominant, we have computed the differential scattering cross section of atomic Rayleigh and nuclear Thomson scattering for the specific case of the most commonly used scatterer Pb ($Z=82$) according to various calculations referred to above. In Fig. 2 we have shown the dependence of $d\sigma(\theta)_{\rm coh}/d\sigma(\theta)_T$ on q over the range $(0.001-10.0)mc$. The results of Florescu-Gavrila[9] are based on their high-energy approximation [Eq. (131) of Florescu-Gavrila[9]] for the scattering of lower-energy photons at finite scattering angles. The results of measurements referred to in Sec. IV are displayed in Fig. 2. It is seen that form-factor theory is sufficient even for high-Z atoms over the q range below $0.5mc$. The RHF form-factor theory is appropriate to scattering of photons with energies greater than the K-shell binding energy of the heavy scatterer atom, whereas for photon energies less than the K-shell binding energy, NRHF form-factor predictions, consistent with new theoretical predictions by Kissel and Pratt are found to show agreement at 5% level below $q=0.2mc$ and within 15% above $q=0.2mc$.

In the q range above $0.5mc$, the Florescu-Gavrila[9] high-energy approximation is sufficient near the low-q end of the observed q distribution for each photon energy over the range 0.400–2.75 MeV, whereas the form-factor theory is sufficient near the high-q end. In the intermediate-q range the distribution of $d\sigma(\theta)_{\rm coh}/d\sigma(\theta)_T$ is in excellent agreement with the prediction of the energy dependence of the Johnson and Cheng[6] exact calculation which agrees with the Florescu-Gavrila[9] and NRHF-RHF results at lower- and higher-q ends, respectively.

This comparison leads to the conclusion that the Florescu-Gavrila[9] high-energy approximation is valid for $(q/\alpha Zm)$ up to 1.6, 2.5, 3.5, 4.3, and 5.7 corresponding to incident photon energies (greater than five times the K-shell binding energy) 0.412, 0.662, 0.889, 1.33, and 2.75 MeV, respectively (here α is the fine-structure constant and m is the electron-rest-mass energy). The corresponding $q/\alpha Zm$ values above which the NRHF-RHF form-factor approximation is adequate are 1.9, 3.5, 5.0, 6.2, and 7.0. For intermediate values of $q/\alpha Zm$ at each of these energies Johnson-Cheng[6] calculations give excellent agreement with the measurements.

ACKNOWLEDGMENTS

The authors wish to thank the University of North Bengal for providing partial support to N. C. Paul, S. K. Sen Gupta, and J. Basu. They are also grateful to Dr. L. Kissel for sending Rayleigh amplitudes and to Dr. J. H. Hubbell for relativistic Hartree-Fock form-factor results.

[1] D. T. Cromer and J. B. Mann, J. Chem. Phys. 47, 1892 (1967); Acta Crystallogr. A 24, 321 (1968).
[2] P. A. Doyle and P. S. Turner, Acta Crystallogr. A 24, 390 (1968).
[3] D. T. Cromer and J. T. Waber, *International Tables for X-ray Crystallography* (Kynoch, Birmingham, 1974).
[4] I. Øverbø, Phys. Lett. B 71, 412 (1977); Nuovo Cimento B 40, 330 (1977).
[5] J. H. Hubbell and I. Øverbø, J. Phys. Chem. Ref. Data (to be published).
[6] W. R. Johnson and K. Cheng, Phys. Rev. A 13, 692 (1976).
[7] H. Cornille and M. Chapdelaine, Nuovo Cimento 14, 1386 (1959).
[8] L. Kissel and R. H. Pratt, Lawrence Livermore Laboratory Report, 1978 (unpublished).
[9] V. Florescu and M. Gavrila, Phys. Rev. A 14, 21 (1976).
[10] B. Sinha, Ph.D. thesis North Bengal University, 1974 (unpublished).
[11] E. Briggs and W. J. Veigele, Kaman Sciences Corp. Colorado Springs, Colo. Report No. K-72-431(SR), 1972 (unpublished).
[12] B. Sinha, S. C. Roy, and N. Chaudhuri, J. Phys. B 9, 3185 (1976).
[13] J. H. Hubbell, W. J. Veigele, E. Briggs, R. T. Brown, and D. T. Cromer, J. Phys. Chem. Ref. Data 4, 471 (1975).
[14] M. Schumacher, F. Smend and I. Borchert, Nucl. Phys. A 206, 531 (1973); 213, 309 (1973); Phys. Rev. C 13, 2318 (1976); Z. Phys. A 283, 15 (1977).
[15] G. Hardie, W. J. Marrow, and D. R. Schwandt, Phys. Rev. C1, 714 (1970); G. Hardie, J. S. Davries, and C. K. Chiang, *ibid.* 3, 1287 (1971).
[16] S. Kahane and O. Shahal, Phys. Lett. B 66, 229 (1977).

J. Phys. B: At. Mol. Phys. **15** (1982) 595–602. Printed in Great Britain

Atomic Rayleigh scattering of photons in the vicinity of K-absorption edges

Swapan K Sen Gupta, Niranjan C Paul, Jahnabi Bose, Gopal C Goswami, Satyendra C Das and Nirmalendu Chaudhuri

Department of Physics, North Bengal University, Darjeeling, 734430 India

Received 8 December 1980, in final form 26 August 1981

Abstract. New measurements of coherent (Rayleigh) scattering of photons of energies in the vicinity of K-absorption edges of gold and lead atoms together with other recent measurements with a coverage in the momentum transfer region up to 1.0 mc are presented for a critical evaluation of (i) the latest relativistic calculation of coherent scattering factors, (ii) the anomalous dispersion correction to the scattering factors and (iii) the exact numerical Rayleigh scattering amplitudes of inner electron shells. This evaluation reveals the ranges of applicability of these calculations and indicates the trend of behaviour due to the proximity of K-absorption edges of scatterer atoms.

1. Introduction

The coherent elastic scattering of x-ray and low-energy gamma rays by bound electrons (Rayleigh scattering) in the vicinity of photoelectric absorption edges of various scatterer elements is a subject of current interest. The region below photon energies of about 100 keV had been of considerable theoretical uncertainty in the past due to the proximity of absorption edges. New theoretical developments (e.g. Kissel and Pratt 1978a, b) for the exact calculation of Rayleigh scattering amplitudes down to photon energies of 100 eV, go beyond the refined relativistic calculations of the form factor (f_0) by Cromer (1965), and the anomalous dispersion corrections, $\Delta f'$ (real) and $\Delta f''$ (imaginary), to f_0 by Cromer and Liberman (1970), for coherent Rayleigh scattering in the nearly forward direction. Below photon energies of 100 keV, the contributions of other elastic scattering processes of the whole atom coherent scattering are negligible compared with that from Rayleigh scattering.

We have measured the angular distribution of the Rayleigh scattering by gold and lead atoms, of photons in the energy region up to 145 keV. In this paper we attempt a presentation of our results, along with the results of other more recent measurements and the latest calculations, in such a way as to exhibit the degree to which the calculations show unity in their predictions with the relatively high-precision experimental data.

2. Measurements

Absolute measurements of the differential coherent atomic scattering cross sections were made as a function of the photon momentum transfer to the bound atomic

0022-3700/82/040595+08$02.00

electrons defined by $q = 2\,k \sin \frac{1}{2}\theta$ in mc units, where k is the incident photon energy in units of the electron rest mass energy and θ is the scattering angle. The experimental set-up and the method of measurements have been described in our previous paper (Sen Gupta *et al* 1978). Only the essentials relevant to our present series of measurements are mentioned. Gamma ray sources include radioactive isotopes ^{141}Ce (145.00 keV), ^{170}Tm (84.30 keV), ^{241}Am (59.54 keV) and ^{210}Pb (47.00 keV), the source strength being in the range 10–100 mCi. The differential cross section measurements have so far been performed for 17 elements. The pulse height spectra were accumulated in a Nuclear Data 1100 multichannel analyser using a storage time of 20–100 ks. In the annular scatterer geometry for nearly forward scattering (figure 1(a)), in addition to the scatterer thickness, radius and source–scatterer distance, three quantities were needed to obtain the total differential cross section: (i) the total number of scattered photons per second, (ii) the total number of photons per second from a similar weak reference source of the same energy and placed at the position of the scatterer and (iii) the background counts per second, all recorded for the same span of time.

The total number of scattered photons was determined by summing over the pulses under the photopeak of the scattered spectrum. The cross section for the coherently scattered photons was obtained by subtracting the incoherently scattered photons determined by the calculations based on the non-relativistic Hartree–Fock (NRHF) scattering functions (obtained from the compilation of Hubbell *et al* (1975)).

For the determination of the cross section at larger scattering angles (figure 1(b)) we separated the coherent peak from the incoherent peak in the scattered spectrum so that the ratio of the number of coherently scattered photons to that of the incoherently scattered photons could be found. This ratio, when combined with the calculated incoherent cross section based on the NRHF incoherent scattering function, yielded the coherent scattering cross section. In the large-angle measurement geometry both the incident and the scattered beams were collimated so that for a very small scatterer in the shape of a right circular cylinder the maximum solid angle between the scatterer and the detector was 5×10^{-2} sr. Corrections due to such a spread of the scattering solid angle are generally small, and were taken into account when necessary. The effect of photons suffering multiple scattering in the target and reaching the detector was also taken into consideration. In the symmetrical-scattering arrangement (figure 1) the photons multiply scattered towards and away from the detector should be mutually compensated to a great extent, therefore, the effect may be neglected since very thin (<200 mg cm^{-2}) scatterers were used.

3. Experimental data and errors

For the presentation intended in this paper we have included the cross sections (table 1) from the set of our completed measurements on Au and Pb for two photon energies (84.30 and 145.00 keV) and have included additional data points for Au and Pb from the following recent high-precision measurements: Schumacher and Stoffregen (1977), photon energy 59.54 keV; Tirsell *et al* (1975), photon energies 25.19, 35.84, 46.00, 55.37 and 74.96 keV; Nath *et al* (1975), photon energy 145 keV; Hauser and Mussgung (1966), photon energy 145 keV.

The total experimental error arising from statistical uncertainties in the background counts, the number of scattered counts and the measurements of relative gamma-ray

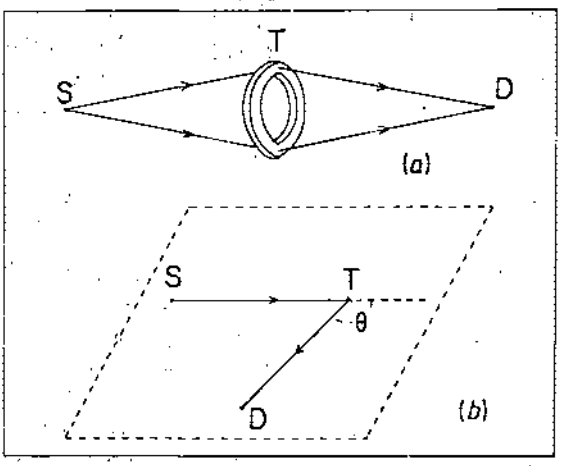

Figure 1. Schematic diagram of the experimental arrangement, (*a*) for small-angle and (*b*) for large-angle scattering measurements. S; source; T, target; D, detector.

Table 1. Measured cross sections for coherent scattering from bound electrons.

Photon energy (keV)	Target (*Z*)	θ	q (mc)	Experimental cross section (b atom^{-1} sr^{-1})
84.30	Au(79)	2°39′	0.008	382.5 (±4.2)[a]
		5°04′	0.015	268.9 (±5.4)
		10°38′	0.030	130.5 (±2.6)
		13°13′	0.038	92.8 (±2.9)
		24°12′	0.069	23.3 (±1.0)
145.00	Pb(82)	1°56′	0.009	418.2 (±12.5)
		2°24′	0.012	267.7 (±8.1)
		3°46′	0.019	279.7 (±8.4)
		8°05′	0.040	92.3 (±4.6)
		13°58′	0.069	54.6 (±3.2)
		15°48′	0.078	33.1 (±2.6)
		19°53′	0.098	23.2 (±2.3)
		24°50′	0.122	12.3 (±1.2)

[a] Figures within parentheses indicate errors in the experimental cross sections.

source strengths was kept in the range from 1% at forward angles to about 10% at intermediate angles. In addition to counting statistics some sources of systematic error were considered in the present measurements. These include uncertainties (i) from the presence of the incoherent component in the measurement of the coherent component, (ii) in the determination of the photopeak area of the coherent component, (iii) from the variation of the detector background in the presence and absence of the scatterer and (iv) in the measurement of source–scatterer distances, scattering angles, thickness of the scatterer and the photon attenuation coefficient for the scatterer. Some of these errors have been either effectively excluded or minimised and others accounted for with appropriate corrections. The correction for the effect (i) was applied with an uncertainty not exceeding 5%. The uncertainty in the cross section due to (ii) was

minimised by using two methods for the evaluation of the photopeak area, the results of which agree to within 2%. The correction for (iii) was at the 1% level and the error in this evaluation was within 10%. The errors in various measurements under (iv) were small and the combined uncertainty in cross section due to these is less than 1%.

4. Rayleigh scattering calculations

The experimental data under consideration represent a significant improvement in precision over earlier coherent scattering measurements and hence deserve careful examination in terms of the latest calculations mentioned in § 1. For this purpose we have computed theoretical differential Rayleigh scattering cross sections in units of the Thomson cross section per electron from the following calculations: the relativistic Hartree–Fock (RHF) calculation of the atomic form factor (f_0) by Doyle and Turner (1968), Cromer and Weber (1974), and Øverbø (1977a, b), obtained from the compilation of Hubbell and Øverbø (1979); the atomic shell-wise calculation of Rayleigh scattering amplitudes by Kissel and Pratt (KP) (1978a, b); and the atomic coherent scattering factors corrected by forward angle dispersion terms by Cromer and Liberman (CL) (1970).

These forward angle dispersion corrections are usually applied (James 1965) at other angles through the use of the following expression

$$\left(\frac{d\sigma}{d\Omega}(\theta)_{coh}\right)\left(\frac{d\sigma}{d\Omega}(\theta)_T\right)^{-1} = \left|f_0+\sum_i \Delta f_i'\frac{f_0^i(q)}{f^i(0)}\right|^2 + \left|\sum_i \Delta f_i''\frac{f_0^i(q)}{f^i(0)}\right|^2 \qquad (1)$$

where $f_0^i(q)$ is the form factor per electron for the ith subshell.

5. Discussion of results

The dependence of the ratio of the coherent (Rayleigh) scattering cross section to the Thomson scattering cross section per electron on the momentum transfer q is shown in figures 2–4 for each of several energies. The results of the measurements referred to in § 3 are displayed in the same figures. At a photon energy of 84 keV no coherent scattering measurements have so far been reported. At 145 keV, the measurements at angles above 30° have been reported by Schumacher (1969). At smaller angles for this energy, the measurements of Hauser and Mussgung (1966) are not consistent with present results or the results of Nath *et al* (1975) and the theoretical predictions based on the dispersion corrected form factor of Pb (figure 3).

When we examine the data points with reference to the respective ratios E_K/E (in the range 0.55–3.20 for Au and 0.6–3.49 for Pb at an interval of 0.1 near $E_K/E = 1$) of the K-edge energy to the incident photon energy E, in different regions of the q distributions, we notice in figure 2 that at photon energies with $E_K/E > 1$ and in the range $0.05 < q < 0.1$, the data points show better agreement with values intermediate between the predictions according to the RHF form factor calculations and the dispersion corrected CL calculations. We also find some indications of explicit dependence on the photon energy beyond $q = 0.1$ (figure 4). The data points with $q < 0.1$ do not show such energy dependence (figure 2) as expected from the fundamental condition of form factor approximation. The points with $E_K/E < 1$ agree with the dispersion corrected CL calculations.

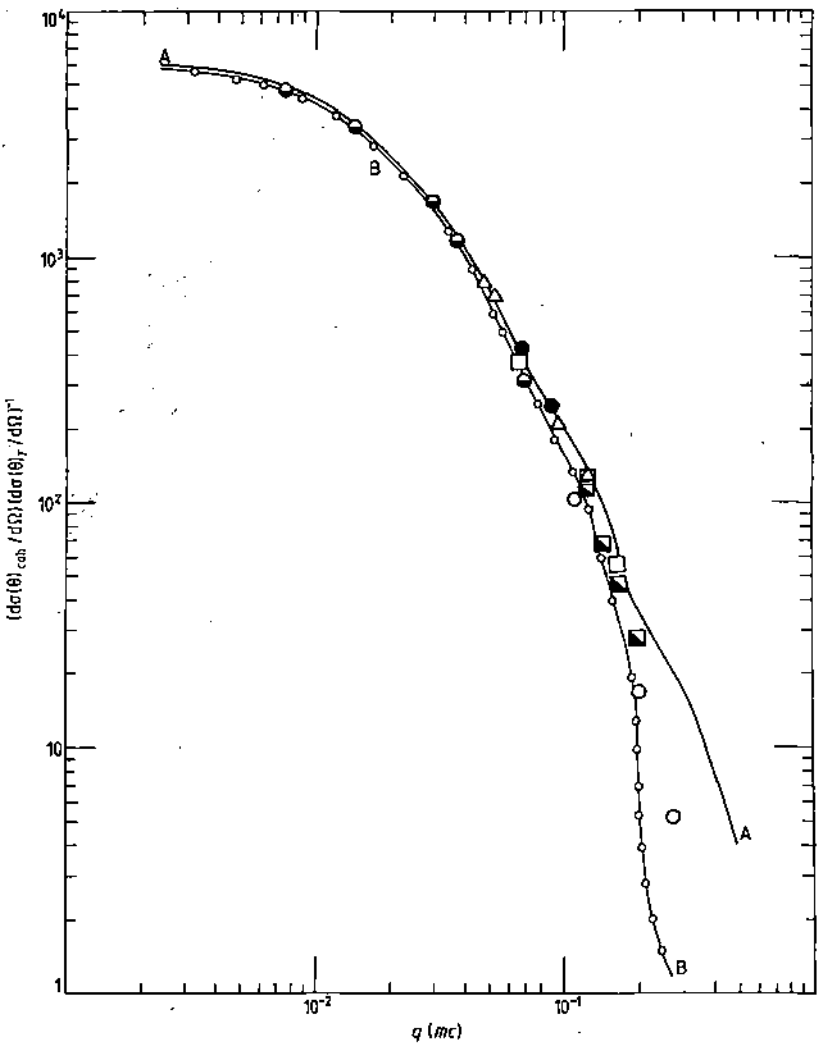

Figure 2. Plot of $(d\sigma(\theta)_{coh}/d\Omega)(d\sigma(\theta)_T/d\Omega)^{-1}$ against momentum transfer, q, in mc units for $Z = 79$. Theoretical predictions: A, form factor ——; B, RHF form factor corrected for dispersion –·–·–. Experimental points: ●, 25.19 keV; △, 35.84 keV; □, 46.00 keV; ◪, 55.37 keV; ○, 74.96 keV (all from Tirsell *et al* 1975); ◒, 145 keV (present measurements).

New theoretical predictions according to the new S-matrix calculation of KP and the results of CL calculations are shown in figure 3 together with the data points with $E_K/E > 1$ and with $E_K/E < 1$. We note a close agreement between these two predictions which agree with the data for several photon energies. At small q below 0.05 and for $E_K/E > 1$, the RHF form factor predictions in close agreement with those of the CL calculations, appear to be the best approximation to the KP prediction.

In order to exhibit the importance of the contributions of higher atomic shells beyond M shells of heavy atoms we plot in figures 3 and 4 shell-wise KP predictions and the data at 35.84, 74.96 and 84.30 keV on Au and at 84.30 and 145 keV on Pb, respectively. We see that below $q = 0.06$ higher-shell contributions are significant and

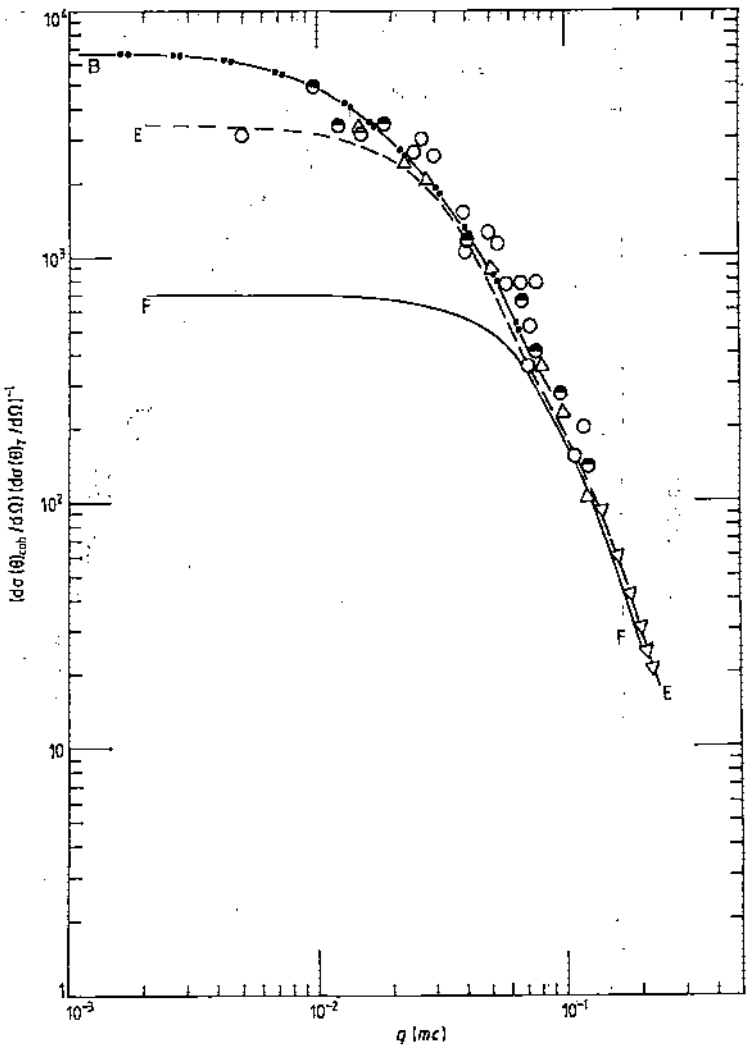

Figure 3. Plot of $(d\sigma(\theta)_{coh}/d\Omega)(d\sigma(\theta)_T/d\Omega)^{-1}$ against momentum transfer, q, in mc units for $Z = 82$. Theoretical predictions: B, Dispersion corrected form factor —·—; E, KP calculation with 59.54 keV for K+L+M+N shells – – –; F, KP calculations using 59.54 keV for K+L+M shells ——. Experimental points: ▽, 59.54 keV (Schumacher and Stoffregen 1977); △, 145.00 keV (Nath *et al* 1975); ○, 145.00 keV (Hauser and Mussgung 1966); ●, 145 keV (present measurements).

have to be included in an exact manner to obtain agreement with data for $E_K/E \geq 1$. Above $q = 0.1$, the sum of the contributions up to the M shell by the S-matrix method is adequate when $E_K/E \geq 1$ for Au and Pb atoms.

In some recent papers (Kissel and Pratt 1978a, b, 1980, Tirsell *et al* 1975, Schumacher and Stoffregen 1977) the experimental data have not been considered for the wider q range, and hence have not been compared with various theoretical predictions as discussed above. This presentation reveals the ranges of agreement and disagreement of various calculations and with the data and is an improvement over previous work.

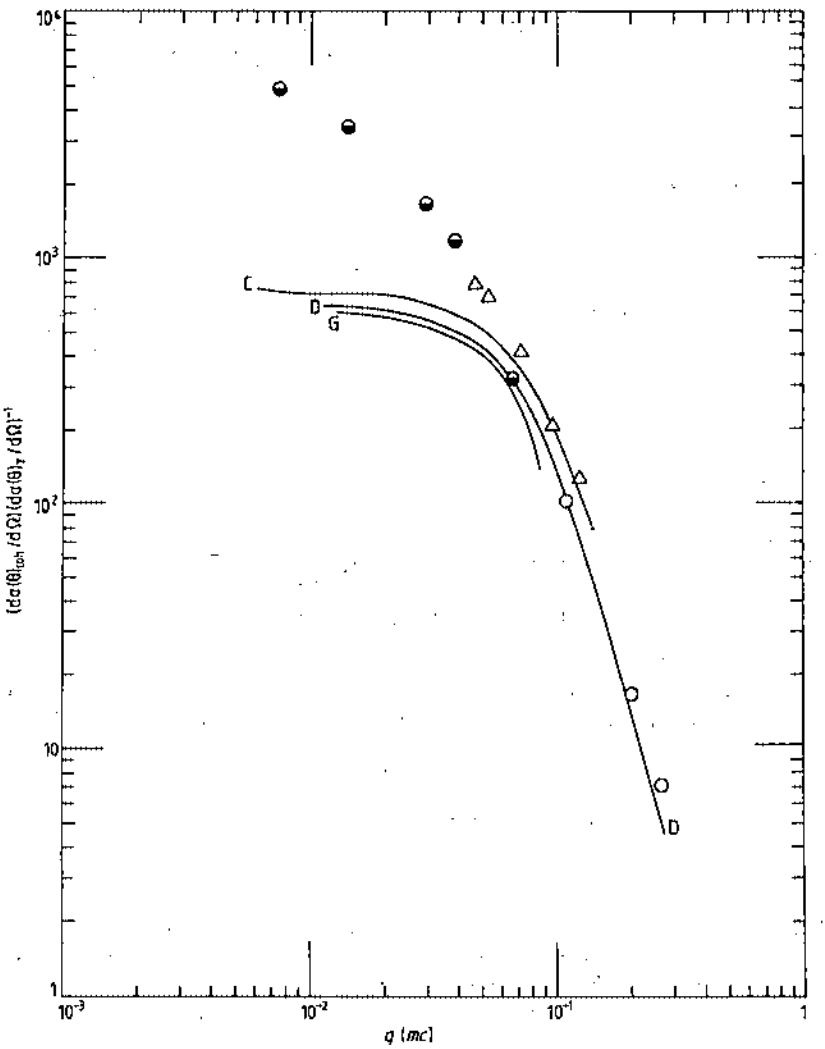

Figure 4. Plot of $(d\sigma(\theta)_{coh}/d\Omega)(d\sigma(\theta)_T/d\Omega)^{-1}$ against momentum transfer, q, in mc units for $Z = 79$. Theoretical prediction: C, KP calculation with 35.84 keV for K+L+M shells ——; D, KP with 74.96 keV for K+L+M shells ——; G, KP with 84.30 keV for K+L+M shells ——. Experimental points: △, 35.84 keV; ○, 74.96 keV (Tirsell *et al* 1975); ◒, 84.30 keV (present measurements).

6. Conclusion

It is now clear that for incident energies below the K edges of heavy atoms the main part of the form factor, f_0, is inadequate above a momentum transfer of 0.2 mc and the dispersion terms $\Delta f'$ and $\Delta f''$ calculated for nearly forward scattering begin to fail for 25.6 keV photons at scattering angles of 172° and at 35° when the incident energy is just below the K edge. The theoretical predictions of Kissel and Pratt (1978a, b) for individual inner electron shells provide the most accurate set now available for a comparison with experimental data above a momentum transfer of 0.06 mc. For lower

values of momentum transfer such exact predictions for outer electron shells are not available and hence there is no other theoretical basis except that of the RHF form factor prediction.

Acknowledgment

The authors wish to express their gratitude to the University of North Bengal for providing UGC Teacher Fellowships to S K Sen Gupta, N C Paul, J Basu and G S Goswami and a Junior Research Scholarship to S C Das. They are also grateful to Dr L Kissel for sending Rayleigh amplitudes and to Dr J H Hubbell, for relativistic Hartree–Fock form factor results.

References

Cromer D T 1965 *Acta Crystallogr.* **19** 224
Cromer D T and Liberman D 1970 *J. Chem. Phys.* **53** 1891
Cromer D T and Weber J T 1974 *International Tables for X-ray and Crystallography* (Birmingham: Kynoch)
Doyle P A and Turner P S 1968 *Acta Crystallogr.* A **24** 390
Hauser U and Mussgung B 1966 *Z. Phys.* **195** 252
Hubbell J H and Øverbø I 1979 *J. Phys. Chem. Ref. Data* **8** 69
Hubbell J H, Veigele W J, Briggs E, Brown R T and Cromer D T 1975 *J. Phys. Chem. Ref. Data* **4** 471
James R W 1965 *The Optical Principles of the Diffraction of X-rays* (Ithaca, NY: Cornell University Press)
Kissel L and Pratt R H 1978a *Phys. Rev. Lett.* **40** 387
—— 1978b *Lawrence Livermore Laboratory Report*
—— 1980 *Lawrence Livermore Laboratory Report*
Nath A, Roy S C and Ghose A M 1975 *Nucl. Instrum. Meth.* **131** 163
Øverbø I 1977a *Phys. Lett.* **71B** 412
—— 1977b *Nuovo Cim.* B **40** 330
Schumacher M 1969 *Phys. Rev.* **182** 7
Schumacher M and Stoffregen A 1977 *Z. Phys.* A **283** 15
Sen Gupta S K, Paul N C, Roy S C and Chaudhuri N 1978 *J. Phys. B: At. Mol. Phys.* **12** 1211
Tirsell K G, Slivnisky V W and Ebert P J 1975 *Phys. Rev.* **12** 2426

Nuclear Instruments and Methods 193 (1982) 395–400
North-Holland Publishing Company

NEW MEASUREMENTS OF COHERENT AND INCOHERENT ATOMIC SCATTERING FACTORS USING RADIOACTIVE GAMMA RAY SOURCES

Swapan K. SEN GUPTA, Niranjan C. PAUL, Jahnabi BOSE, Satyendra C. DAS and Nirmalendu CHAUDHURI

Department of Physics, University of North Bengal, Pin 734430, Darjeeling, India

A representative sample of results of our measurements over the photon energy range 0.08–2.00 MeV on coherent and incoherent scattering is presented and compared with theoretical predictions resulting from new calculations at photon energies below and above the K-shell binding energy of heavy atoms. The present results taken with some other recent measurements near and far from K-absorption edges of the scatterer atom help identify the region in photon energy and momentum transfer for the applicability of various theoretical predictions for photon coherent scattering. The Hartree–Fock model for bound electron incoherent scattering is found to be adequate in explaining the measured whole atom incoherent scattering factors over the whole momentum transfer range investigated.

1. Introduction

We have made a series of precision measurements of the scattering of photons over the energy range 0.080–2.00 MeV. In this paper we make a presentation of present results of coherent and incoherent scattering of photons for a number of representative low, medium, and high Z atoms together with some results of other measurements in such a way as to indicate the degree to which these measurements serve as a test of the various calculations.

2. Measurement

Absolute measurements of the differential atomic scattering cross sections were made as a function of photon momentum transfer to the bound atomic electrons defined by $q = 2k\,\mathrm{sim}(\theta/2)$ where k is the incident photon energy in units of electron rest-mass energy, and θ is the scattering angle [1]. The essentials relevant to the present measurements in the symmetrical scattering arrangements (fig. 1) are mentioned. The gamma ray sources included radioactive isotopes ^{201}Pb (47 keV), ^{241}Am (59.54 keV), ^{170}Tm (84.30 keV), ^{141}Ce (145 keV), ^{203}Hg (279.2 keV), ^{137}Cs (662 keV), ^{65}Zn (1.115 MeV), ^{60}Co (1.17 and 1.33 MeV) and ^{124}Sb (2.09 MeV), the source strength being in the range 3 mCi for ^{241}Am to 750 mCi for ^{124}Sb, the differential cross section measurements were done for 15 elements representing low, medium and high Z atoms. At scattering angles above 15° (fig. 1b), we separated the coherent peak from the incoherent peak in the scattered spectrum using suitable NaI (Tl) detectors. The pulse height spectra were accumulated in a ND1100 multichannel analyzer.

3. Results: theoretical and experimental

3.1. Coherent scattering

We have measured coherent scattering from a number of low, medium, and high Z represen-

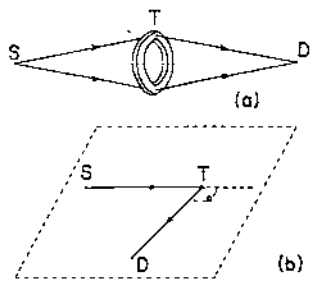

Fig. 1. Schematic diagram of the experimental arrangement for (a) small, and (b) large-angle scattering measurements. S–source, T–target, and D–detector.

0029-554X/82/0000–0000/$02.75

tative elements covering a momentum-transfer range (0.001–0.15)mc. The results of measurements presented here are of energy 0.145 MeV (fig. 2), 0.662 and 1.33 MeV (fig. 3). The differential cross sections have been computed using $F(q,z)$ values based on nonrelativistic Hartree–Fock (NRHF) wave functions [2, 3]. In fig. 4 we have shown the dependence of $[d\sigma(\theta)_{coh}/d\Omega]/[d\sigma(\theta)_T/d\Omega]$ (i.e. $|F(q,z)|^2$) for Pb on q over the range (0.001–10)mc. In addition to the data points from our own measurements on Pb we have included in fig. 4 the data points for Pb from other recent measurements of (1) Schumacher et al. [4], photon energies 412 keV (eight data points), 622 keV (seven data points), 889 keV (nine data points), 1.12 MeV (nine data points) and 2.75 MeV (eight data points); (2) Hardie et al. [5], photon energy 1.33 MeV (ten data points); (3) Kahane et al. [6], photon energy

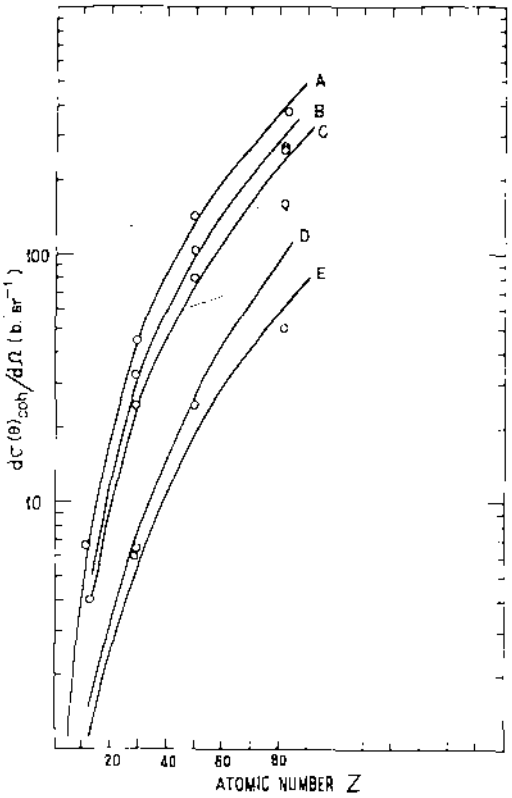

Fig. 2. Experimental scattering cross sections $d\sigma(\theta)_{coh}/d\Omega$ (in b.sr^{-1}) with 0.145 MeV photons (A) for $q = 0.0095mc$, (B) for $q = 0.014mc$, (C) for $q = 0.019mc$, (D) for $q = 0.04mc$ and (E) for $q = 0.05mc$ compared with predictions from $d\sigma(\theta)_{coh}/d\Omega = d\sigma(\theta)_T/d\Omega . F(q, z)|^2$ (i.e. coherent).

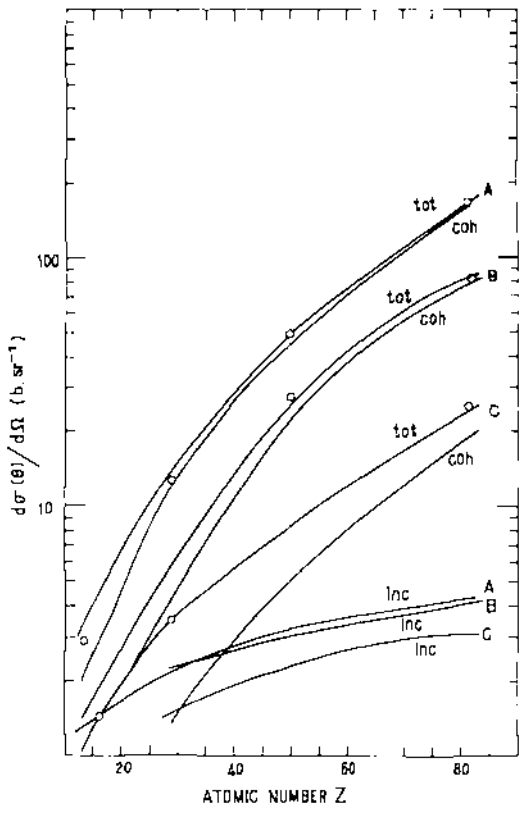

Fig. 3. Experimental scattering cross section, $d\sigma(\theta)_{tot}/d\Omega$ (in b·sr^{-1}) with 0.662 MeV photons (A) for $q = 0.027mc$, with 1.33 MeV photons (B) for $q = 0.045mc$ and (C) for $q = 0.09mc$ compared with $d\sigma(\theta)_{coh}/d\Omega = d\sigma(\theta)_T/d\Omega|F(q, z)|^2$ (i.e. coherent) and $d\sigma(\theta)_{inc}/d\Omega = d\sigma(\theta)_{KN}/d\Omega S(q, z)$ (i.e. incoherent). tot is the sum of the coherent and incoherent

6.84 MeV (one data point). The data points for photons in the energy range 25–145 keV are displayed in figs. 5 and 6. The theoretical predictions for the differential cross section in units of Thomson cross section per electron have been obtained from the following calculations: (1) NRHF form factor by Cromer and Mann [2], compiled by Hubbell et al. [3]; (2) relativistic Hartree–Fock (RHF) calculation of the atomic form factor by Doyle and Turner [7], Cromer and Weber [8] and Øverbø [9], compiled by Hubbell et al. [10]; (3) atomic shell-wise calculation of the Rayleigh scattering amplitudes by Johnson and Cheng [11], Cornille and Chapdeline [12], and Kissel and Pratt (KP) [13]; (4) atomic K-shell Rayleigh scattering amplitudes by Florescu and Gavrila [14]; and (5) atomic coherent scattering factors corrected for

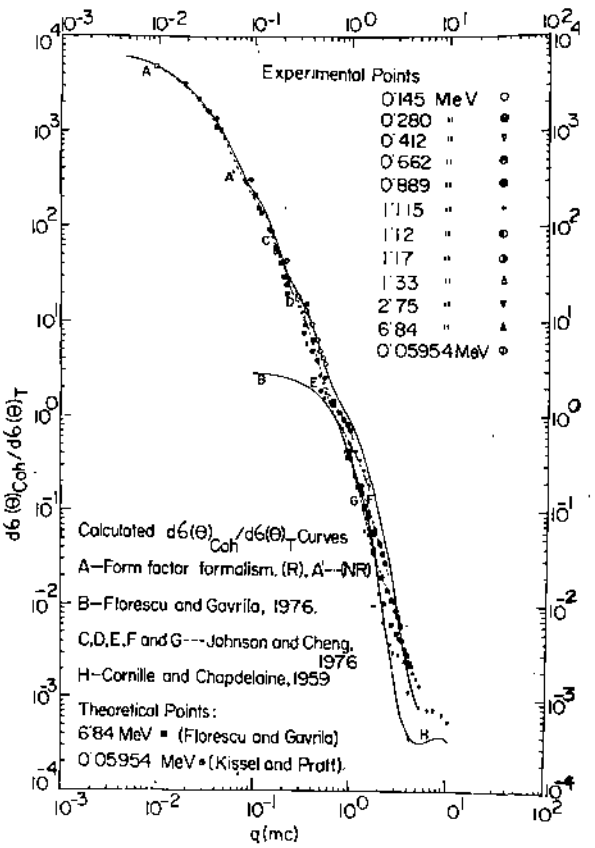

Fig. 4. $[d\sigma(\theta)_{coh}/d\Omega]/[d\sigma(\theta)_T/d\Omega]$ plotted versus $q(mc)$.

forward angle dispersion terms by Cromer and Liberman (CL) [15].

3.2. Incoherent scattering at small momentum transfer

We have taken measurements of a number of selected atoms with $Z = 5$, 6, 7, 11, 13, 16, 21, 26, 29, 30, 50, 74, 79, 80, and 82 covering a momentum transfer range $(0.3–0.12)mc$ using nearly monoenergetic photon beams over an energy range 0.5–2.0 MeV. The completed measurements included here for presentation are atoms of $Z = 13$, 16, 29, 50, and 82 for photons of energies 0.662 and 1.33 MeV. The results are presented in figs. 3, 7 and 8. In figs. 3 and 7 the coherent scattering has not been subtracted from the experimental total cross section measurements in order to compare more clearly the measurements and predictions in the small momentum transfer region, where the binding effect is important.

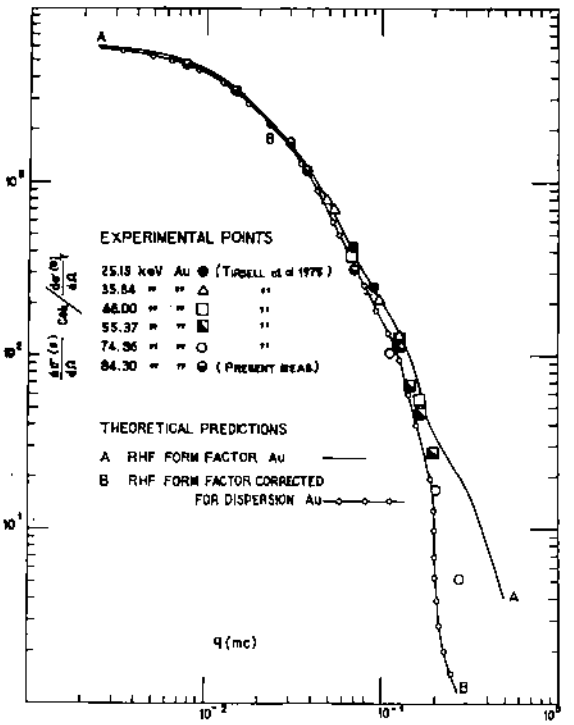

Fig. 5. Plot of $[d\sigma(\theta)_{coh}/d\Omega]/[d\sigma(\theta)_T/d\Omega$ versus momentum transfer q in units of mc for $Z = 79$. Theoretical predictions: (A) form factor (solid line); (B) RHF form factor corrected for dispersion of line width small circles). Experimental points: ● 25.19 keV, △ 35.84 keV, □ 46.00 keV ▪ 55.37 keV, ○ 74.96 keV (all from Tirsell [16]); ● 84.30 keV (present measurements).

4. Discussion and conclusions

The new results of coherent scattering cross sections for representative low, medium, and high Z atoms over photon energies of 0.145–1.33 MeV are considered in figs. 2 and 3 with a basic interpretation of form factor approximation based on the HF model calculation of $F(q, z)$ [3], which adequately interprets measured atomic scattering factors over a momentum-transfer range $(0–0.15)mc$. The interpretation of the data over a wider momentum-transfer range for the scattering of photons up to several MeV is considered in fig. 3 in terms of various theories mentioned in section 3.1. It is seen that the form factor theory is appropriate to scattering of photons with energies greater than the K-shell binding energy of the heavy scatterer atoms.

In the q range above $0.5mc$ (fig. 4) the Florescu–Gavrila [14] high energy approximation

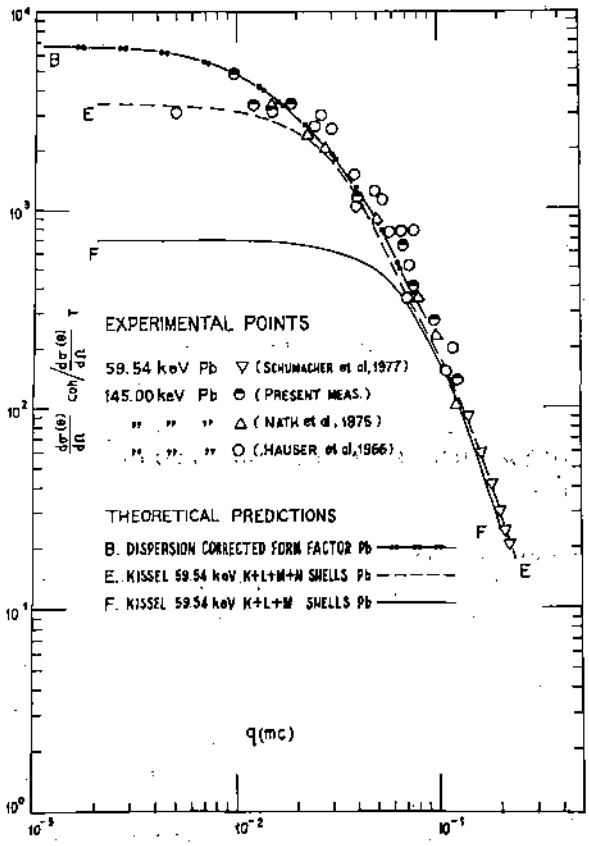

Fig. 6. Plot of $[d\sigma(\theta)_{coh}/d\Omega]/[d\sigma(\theta)_T/d\Omega]$ vs momentum transfer q in mc units for $Z = 82$. Theoretical predictions: (B) dispersion corrected form—·—·—; (E) KP calculations with 59.54 keV for K + L + M + N shells - - - ; (F) KP calculations using 59.54 keV for K + L + M shells—. Experimental points: ▽ 59.54 keV (Schumacher [4]); △ 145.00 keV (Nath [17]); ⊖ 145.00 keV (Hauser [18]); ⊖ 145.00 keV (present measurements).

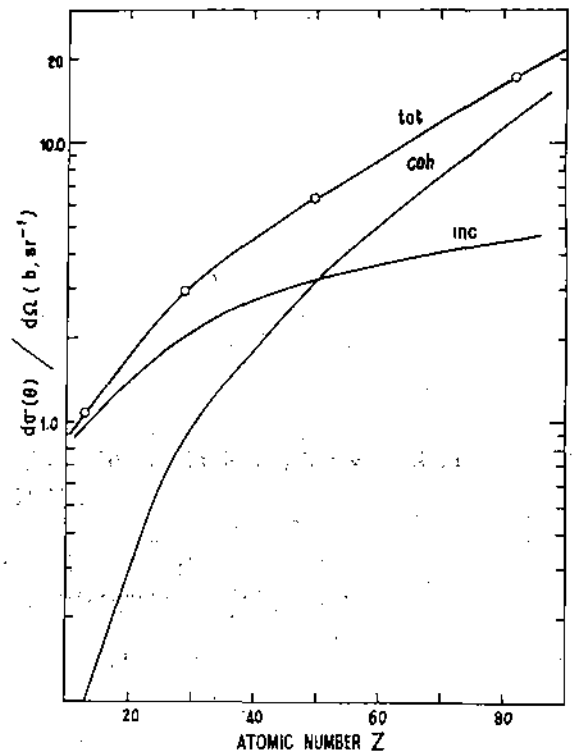

Fig. 7. Experimental scattering cross section (○) of 0.662 MeV photons at $q = 0.107mc$ with predictions inc, coh and tot as in caption of fig. 3.

is sufficient near the low q end of the observed q distribution for each of the photon energies over the range 0.400–2.75 MeV, whereas the form factor theory is sufficient near the high q end. In the intermediate q range the distribution of $[d\sigma(\theta)_{coh}/d\Omega]/[d\sigma(\theta)_T/d\Omega]$ is in excellent agreement with the prediction of the energy dependence of the Johnson and Cheng [11] exact calculation, which agrees with Florescu–Gavrila [14] and NRHF–RHF results at lower and higher ends, respectively. This leads to the conclusion that the Florescu–Gavrila high energy approximation is valid for $q/\alpha Zm$ up to 1.6, 2.5, 3.5, 4.3 and 5.7 corresponding to incident photon energies (greater than five times the K-shell binding energy of high Z atoms) 0.412, 0.662 0.889, 1.33 and 2.75 MeV, respectively (here α is the fine structure constant and m is the electron rest-mass energy). The corresponding $q/\alpha Zm$ values above which the NRHF–RHF form factor approximation is adequate are 1.9, 3.5, 5.0, 6.2 and 7.0. For intermediate values of $q/\alpha Zm$ at each of these energies, the Johnson and Cheng calculations give excellent agreement with the measurements.

At photon energies below and near the K-shell binding energies of scatterer atoms the data are considered in figs. 5 and 6. In reference to the respective ratios E_k/E (in the range 0.55–3.20 for Au and 0.6–3.49 for Pb at an interval of 0.1 near $E_K/E = 1$) of the K-edge energy to the incident photon energy, E, in different regions of q-distributions, we notice in fig. 5 that at photon energies with $E_k/E > 1$ and in the range $0.05 < q < 0.1$, the data points show better agreement with values intermediate between the predictions of the RHF form factor calculations and dispersion corrected CL calculations. We also find some indications of explicit dependence on the

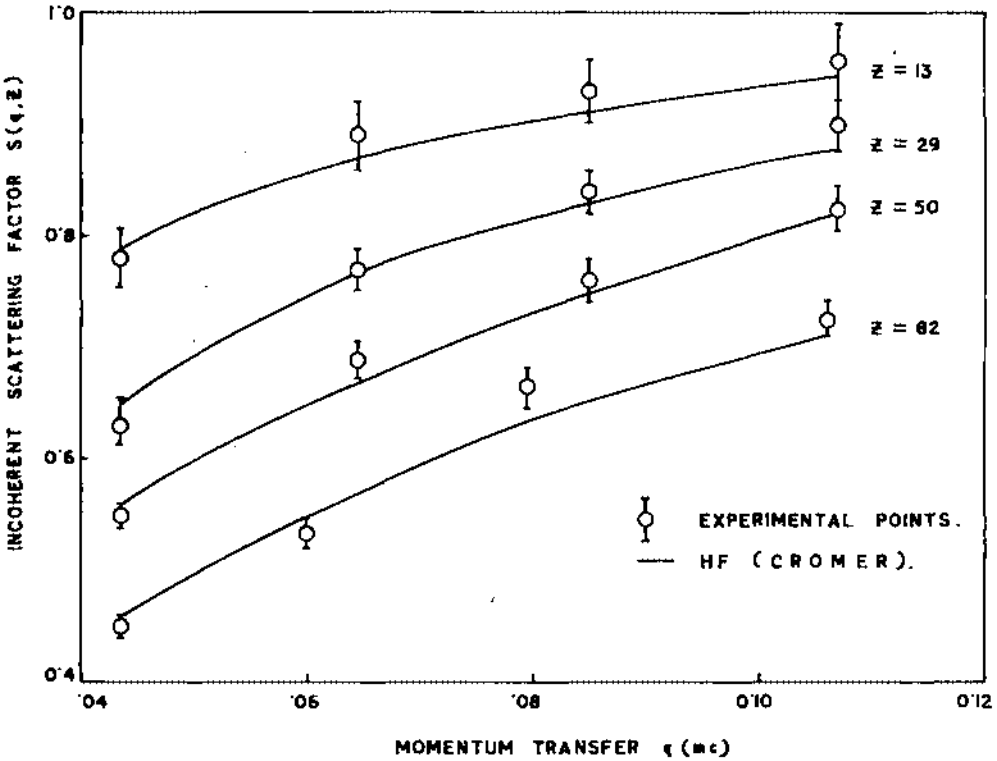

Fig. 8. Incoherent scattering factor vs. momentum transfer. Present measurements (circles with error bar) compared with calculations based on NRHF model [3].

photon energy beyond $q = 0.1$ (fig. 6). The data points with $q < 0.1$ do not show such energy dependence (fig. 5) as expected from the fundamental condition of form factor approximation. The points with $E_k/E < 1$ agree with dispersion corrected CL calculations. New theoretical predictions according to the new S-matrix calculation of KP and the results of CL calculations are shown in fig. 6 with the displaying of the data points with $E_k E > 1$ and $E_k/k < 1$. We note a close agreement between these two predictions which agree with the data for several photon energies. At small q below 0.05 and for $E_k/E > 1$, the RHF form factor prediction in close agreement with those of CL calculations appears to be the best approximation to KP predictions. In some recent papers [4, 5, 13], the experimental data have not been considered for a wider q range and have not been compared with various theoretical predictions discussed above. This presentation reveals the ranges of agreement of various calculations with the data and is an improvement over previous work.

The present data on $S(q, z)$ for low, medium, and high Z atoms (fig. 8) over the momentum transfer range (0.03–0.12)mc are seen to be in reasonable agreement with incoherent scattering function approximations based on the configuration interaction (Brown [18]) and new HF wave functions [2]. This means that the effect of electron binding which is effectively revealed at low momentum transfer ($q < 0.1$) incoherent scattering processes is accounted for satisfactorily.

The authors are grateful to North Bengal University and U.G.C., Govt. of India.

References

[1] B. Sinha, S.C. Roy and N. Chaudhuri, J. Phys, B: At. Mol. Phys. 9 (1976) 3185.
[2] D.T. Cromer and J.B. Mann, J. Chem. Phys. 47 (1967) 1892; Acta Crystallogr. A24 (1968) 321.
[3] J.H. Hubbell, W.J. Veigele, E. Briggs, R.T. Brown and D.T. Cromer, J. Phys. Chem. Ref. Data 4 (1975) 471.
[4] M. Schumacher, F. Smend and I. Borchert, Nucl. Phys. A206 (1973) 531; A213 (1973) 309; Phys. Rev. C13 (1976) 2318; Z. Physik. A283 (1977) 15.

[5] G. Hardie, W.J. Marrow and D.R. Schwandt, Phys. Rev. C1 (1970) 714; G. Hardie, J.S. Davries and C.K. Ciang, ibid. C3 (1971) 1287.
[6] S. Kahane and O. Shahal, Phys. Lett. B66 (1977) 229.
[7] P.A. Doyle and P.S. Turner, Acta Crystallogr. A24 (1968) 390.
[8] D.T. Cromer and J.T. Waber, Intern. tables for X-ray crystallography (Kynoch, Birmingham, 1974).
[9] I. Øverbø, Phys. Lett. B71 (1977) 412; Nuovo Cim. B40 (1977) 330.
[10] J.H. Hubbell and I. Øverbø, J. Phys. Chem. Ref. Data 8 (1979) 69.
[11] W.R. Johnson and K. Cheng, Phys. Rev. A13 (1976) 692.
[12] H. Cornille and M. Chapdeline, Nuovo Cim. 14 (1959) 1386.
[13] L. Kissel and R.H. Pratt, Phys. Rev. Lett. 40 (1978) 387; Lawrence Livermore Lab. rep. (1978) and (1980).
[14] V. Florescu and M. Gavrila, Phys. Rev. A14 (1976) 21.
[15] D.T. Cromer and D. Liberman, J. Chem. Phys. 53 (1970) 1891.
[16] K.G. Tirsell, V.W. Slivnisky and P.J. Ebert, Phys. Rev. 12 (1975) 2426.
[17] A. Nath, S.C. Roy and A.M. Ghose, Nucl. Instr. and Meth. 131 (1975) 163.
[18] U. Hauser and B. Mussgung, Z. Physik 195 (1966) 252.
[19] B.J. Bloch and L.B. Mendelsohn, Phys. Rev. A9 (1974) 129.

REQUEST
Author, please indicate
• printer's errors in BLUE
• author's changes in RED

North-Holland Publishing Company
Aantal pagina's
1 t/m 5

17D-2
1e proef

Artikelnummer
Nim 01250

5 MEI 1982

Nuclear Instruments and Methods 00 (1982) NIM 01250
North-Holland Publishing Company

A SIMPLE METHOD OF STUDYING ATOMIC SCREENING EFFECTS IN PAIR PRODUCTION

Jahnabi BOSE, Swapan K. SEN GUPTA, Niranjan Ch. PAUL, Gopal Ch. GOSWAMI, Saty[illegible]a C. DAS and Nirmalendu CHAUDHURI

Department of Physics, North Bengal University, Darjeeling-734430, India

Received 1 December 1981

The development of a simple method for an atomic pair production experiment is described. The preliminary results obtained by removing various experimental difficulties and errors are presented to justify the suitability of the method over other more expensive pair detection systems reported in recent literature.

1. Introduction

The method used in the measurement of pair production cross sections in the sixties used NaI(Tl) detectors in the coincidence technique. The results of these measurements are now found to be not adequately reliable for a comparison with more refined theoretical calculations taking screening correction to the pair production into account. The experimental method of Avignone et al. [1] using a spherical symmetry of the target and source is dependent on experimental values of the annihilation pair production detection efficiency and the total gamma-ray absorption coefficient of the target material and is subject to experimental uncertainties. Another disadvantage of the method arises from the poor statistics due to the lower detection efficiency of the Ge(Li) detector.

The present paper describes a method of measuring pair production cross sections and has the following advantages: (1) separate measurements of the annihilation pair production detection efficiency is not needed in the evaluation of the cross section relative to a standard cross section; (2) the total gamma-ray absorption coefficients of the target material do not enter into the computation of the cross section; (3) a large number of corrections to the data is avoided; (4) a resolving time of about 40 ns has been achieved by improved electronics; (5) the continuum background does not affect the result and there is no problem in the analysis of very well defined simple pair annihilation peaks obtained by a NaI(Tl) detector; (6) the method is suitable for testing new theoretical screening corrections to the pair production cross section.

Preliminary results of cross section measurements by this method on three elements ($Z = 29$, 50 and 79) using photons of energies 1.1732 and 1.3325 MeV from a ^{60}Co source are also discussed.

2. Method

2.1. Formulation

The idea of this experiment is to obtain cross section results by avoiding the determination of various experimental factors and errors in counting, in coincidence, of two annihilation-quanta produced when the positrons of the pairs created in the target stop and annihilate with electrons. The target chosen was thick enough to stop the positrons but thin for the incident gamma-ray beam. When observing the two annihilation-quanta at 180° apart created in a target 'X' of atomic number Z, the spectrum of annihilation photons at the given direction with respect to the incident gamma-ray beam was recorded along with that from an exactly similar lower Z comparison radiator (taken as standard) placed at the same position of X, in exactly the same geometry.

The intensity of the annihilation-quanta determined from the area of the photopeak of the sample target X was compared with that in the spectrum of the standard radiator. The standard radiator element chosen was copper ($Z = 29$) because this gives counted annihilation-quanta of better statistics and the effect of trident production and incoherent pair production is negligibly small at such intermediate atomic number elements. Taking copper as the standard radiator this procedure gives for the cross section ratio

$$\frac{\sigma_X}{\sigma_{Cu}} = \frac{C_X A_X}{C_{Cu} A_{Cu}}, \qquad (1)$$

where C_X and C_{Cu} are the intensities of the annihilation radiation per g cm^{-2} of the thin sample radiator X and the standard radiator (copper); A_X and A_{Cu} are the atomic weights of the sample target X and the standard radiator, respectively.

2.2. Procedure and technique

An improvement in measurements of two-photon annihilation events, 180° apart, has been achieved by eliminating effects due to (1) absorption of annihilation-quanta in the target, (2) absorption of incident photons in the target, (3) backgrounds (chance and false coincidences) resulting from interactions other than pair production in the target and background materials, and (4) the effect of short-term variation of the detection efficiency of annihilation photons.

The corrections arising from the effects (1) and (2) have been eliminated by measuring the coincidence rate of two-photon annihilation radiation from varying thicknesses of the sample targets. Targets of copper, tin and gold were taken in the form of circular foils 2 cm in diameter and were placed as shown in fig. 1. They have identical geometry with respect to source and detectors. Target thicknesses from about 0.067 g cm^{-2} to a maximum of 0.62 g cm^{-2} were used in the measurements. To minimise the effects (3) and (4) the data were taken alternatively on each set of standard and sample targets in the following sequence: standard target (coincidence rate at 180° and at 90° between the axes of the two detectors), sample targets (coincidence rate at 180° and 90° positions of the two detectors), background coincidences at the two positions with and without target, standard targets, and so on. The counting time for the sequence was adjusted to obtain a satisfactory statistical error level. The shapes of the background spectrum without target at 180° and 90° positions are found to be exactly identical. The sample and 'standard' coincidence rate at the 90° position have been taken as the chance coincidence rate in the determination of the pair annihilation coincidence rate at 180° position and has been used to correct the observed coincidence spectrum. A selection of background and observed annihilation spectra at 180° is shown in fig. 2. The true coincidence rates for various thicknesses of each element of the pair thus determined were found to fit an expression

$$N = C\, t\, e^{-at}, \qquad (2)$$

where t is the target thickness in g cm^{-2}, and C is the true two-photon coincidence count rate for a target of thickness 1 g cm^{-2} and a is a constant for a given element. The constants C and a were determined through a proper fitting procedure. The obtained fits to the data for three elements are shown in fig. 3.

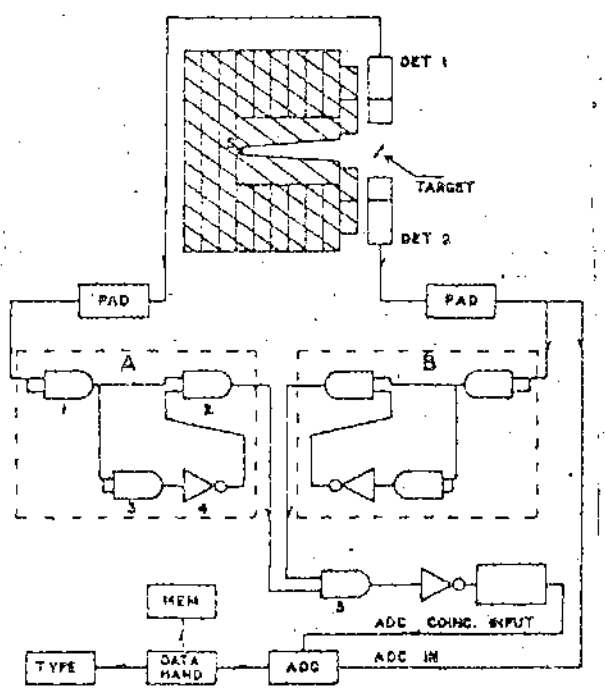

Fig. 1. Experimental arrangement showing source–target–detector geometry along with block diagram of the associated electronics.

2.3. The coincidence circuit

The electronics shown as a block diagram in fig includes a coincidence system having a resolving time of about 40 ns. The output resulting from the coincidence between the two detectors was used to gate a multichannel analyser (MCA) which recorded the 0.51 MeV annihilation radiation spectrum from one of the detectors. The gamma ray source used was a 300 mCi ^{60}Co (1.1732 and 1.3325 MeV) cylindrical pallet placed in a 30 cm deep and 1.8 cm diameter bored lead block. The minimum thickness of lead shielding at the sides and at the back of the source was 35 cm. The gain and biases of the two PADs of the MCA and the high voltage supply to each photomultiplier tube of the two detectors (Det 1 and Det 2) were set so that energy calibration of the channels was the same for both detectors. A pulse detected by either detectors after being amplified by the respective PADs was fed into two separate pulse shaping circuits A and B. The amplified pulse from a PAd was applied to the shorted terminals of a dual input AND gate 1. The output from this gate was applied simultaneously to one input terminal of another dual input AND gate 2 and to a shorted input terminal of a dual input AND gate 3. The output from gate 3 is inverted by an inverter gate 4 and applied to the other input terminal of AND gate 2. The input logic levels of the input terminals of gate 2 were adjusted so that the gate gave output until a pulse from the inverter gate 4 is approximately 40 ns. Therefore, whatever be the pulse width of the output of the PAD, there was always an output pulse at the output of gate 2 with a width of 40 ns. A pulse of similar width was also obtained from the identical circuit for the other detector. These two pulses

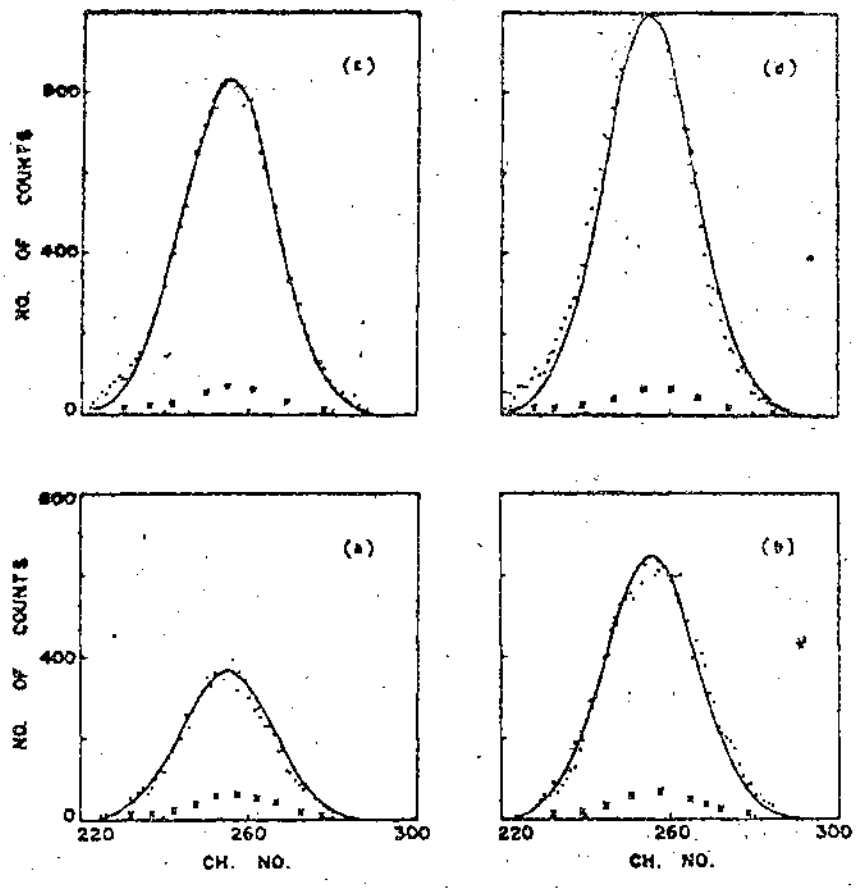

Fig. 2. Observed annihilation spectra for gold at 180° position showing observed counts (dotted line), fitted curve (full line), and background counts (crosses); (a), (b), (c) and (d) give the above spectra of increased thickness.

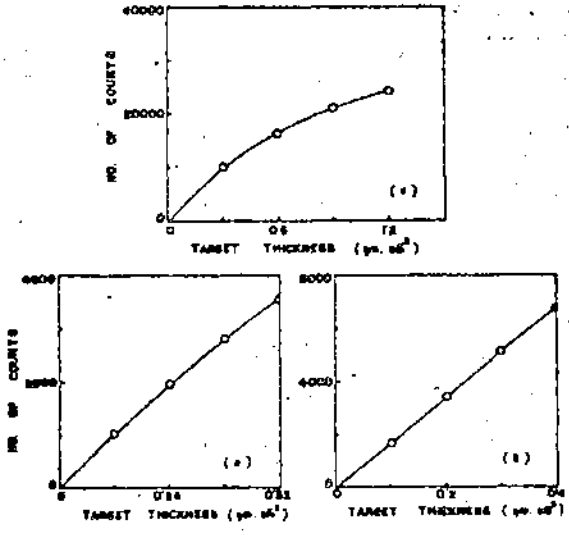

Fig. 3. Observed total counts (circles) plotted against target thickness (g cm^{-2}). Full line, fitted curve according to eq. (2). (a), (b) and (c) for copper, tin and gold, respectively.

of width 40 ns were applied to the input terminals of a dual input AND gate 5. This gate would give an output only when its inputs arrive within 40 ns. This output was inverted and applied to the monostable multivibrator with Schmitt-trigger input. The external timing capacitor and resistor were adjusted to obtain a pulse of proper height and width which was applied to the coincidence input of the ADC of MCA. The output pulse of Det 2 was fed through PAD to the ADC input for analysis enabling it to give a pulse spectrum from Det 2 which is in coincidence with Det 1, with a given a time resolution.

3. Errors

The present measurements are free from some of the possible uncertainties because the ratio of the two annihilation radiation peak counts in identical geometry has been taken. These uncertainties include systematic errors arising from (1) the limited energy resolution of

Table 1
Theoretical and experimental pair production cross section ratios.

Ratio	Theoretical				Experimental					
	Born approx.	Øverbø [2] (Pe)	Øverbø [2] (Se)	Tseng [3] Pratt (Se)	Girard[4] et al.	Dayton [5]	Standil [6]	Schmidt [7]	Present Expt.	Henry et al. [8]
σ_{Sn}/σ_{Cu}	2.97	3.83	3.95	3.93	3.85	3.66	3.48	3.47	3.97 ± .15	
σ_{Au}/σ_{Cu}	7.40	12.74	14.00	13.68	–	–	–	–	14.13 ± .33	
σ_{Pb}/σ_{Cu}	7.99	13.86	15.56	15.12	15.33 ± 0.92	14.70	13.93	13.69		15.29 ± .11
σ_{U}/σ_{Cu}	10.07		21.52	20.79	21.4 ± 1.32					

Table 2
Theoretical and experimental pair production cross sections in mb. atom^{-1} at energies 1.1732 and 1.3325 MeV.

Element	Theoretical				Present experimental, taking the cross section value of copper as					
	Born approx. Born	Øverbø [2] (Pe)	Øverbø [2] (Se)	Tseng, [3] Pratt (Se)	10.10 from ref. 2	10.00 from ref. 3	Other experiments			
							ref. 7	ref. 4	ref. 5	ref. 6
Sn	24.03	38.20	39.90	39.50	40.17 ± 1.54	39.70 ± 1.54	32.68	40.5 ± 2	35.9	33.16
Au	59.82	126.83	141.40	136.83	142.71 ± 3.22	141.30 ± 3.22				
Pb	64.66	137.9	157.2	151.2				161 ± 6		
U	81.36		217.3	307				222 ± 9		

Pe – Point Coulomb approximation Cross section.

Se – Screening corrected Cross section.

NaI(Tl) detectors, (2) measurement of the efficiency of detection of annihilation radiation, (3) measurement of activity of primary photon source, (4) the shape of the targets and source–target–detector geometry. Since the data were recorded alternatively on the standard and sample target of identical shape of cylindrical symmetry the errors involved due to (1)–(4) remained constant and did not affect the ratio of two annihilation peaks. As already mentioned in sect. 2.2, the corrections were applied to the 180° coincidence rate for background coincidence, chance coincidences and attenuation of incident and annihilation photons in the standard and sample targets.

4. Results and discussion

The results obtained from measurements using a gamma-ray source of mixed photon energies on pure copper (standard), tin and gold targets are given in table 1 together with cross section ratios as obtained from some recent direct measurements and latest theoretical predictions in fig. 4. The area ratio of two annihilation peaks yields the absolute value of the pair production cross section for the target atom because the pair production cross section of standard copper atom is given to a high degree of accuaracy. This standard cross section at the mixed ^{56}Co gamma-rays is 10.10 mb according to Øverbø [2] and 10.00 mb according to Tseng and Pratt [3]. Taking these values in our experimental values of cross section ratios of table 1, the extracted experimental cross section values of tin and gold are given in table 2, together with some other experimental results [4–8]. The present results are free from any systematic errors which may occur in the measurements because here a ratio of two peak areas is determined.

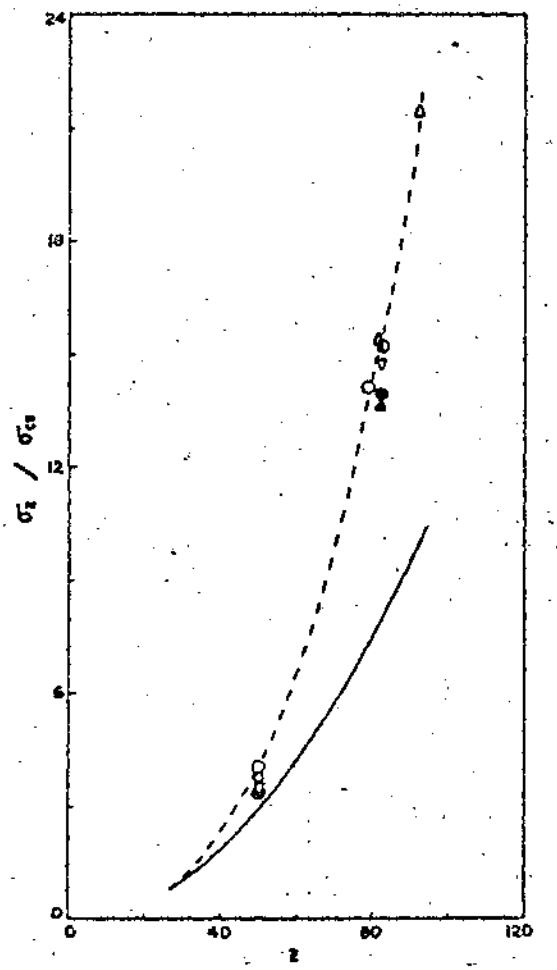

Fig. 4. Graphs showing σ_Z/σ_{Cu} vs. Z, according to the Born approximation (full line), according to the screening correction of Øverbø [2] (dashed line). Experimental points; △ Girard et al. [4], ▽ Dayton [5], ● Standil et al. [6], ▲ Schmidt et al. [7], ◐ Henry et al. [8], ○ our experiment.

The effect of screening on the cross section of pair production near threshold is important for atoms of larger atomic number. The screening effect for higher Z target atoms can be checked relative to that for a standard intermediate Z atom (copper) for which the screening correction is small, theoretically well known and the cross section is not negligibly small. As demonstrated in fig. 4 it is easier to check experimentally the screening correction in the presently adopted method that avoids various sources of errors which were found to be very difficult to remove in earlier direct experiments [1,4]. Most of the recent experiments used Ge(Li) detectors which give a lower counting efficiency resulting in poor statistics.

The results presented in this paper thus demonstrate the suitability of the present method in making a direct experimental check on the screening correction for pair production in high Z target atoms at energies very near to threshold.

The authors are grateful to the University of North Bengal for providing U.G.C. Teacher Fellowships to J. Basu, N.C. Paul, S.K. Sen Gupta and G.C. Goswami and a Junior Research Fellowship (UGC) to S.C. Das.

References

[1] F.T. Avignone III and S.M. Blankenship, Nucl. Instr. and Meth. 116 (1974) 515.
[2] I. Øverbø, Physica Scripta 19 (1979) 299; Thesis work (1967) (unpublished).
[3] H.K. Tseng and R.H. Pratt, Phys. Rev. A 6 (1972) 2049.
[4] T.A. Girard, F.T. Avignone III and S.M. Blankenship, Phys. Rev. A 17 (1978) 218; Phy. Lett. 71A (1979).
[5] I.E. Dayton, Phys. Rev. 89 (1953) 544.
[6] S. Standil and V. Shkolnik, Can. J. Phys. 36 (1958) 1154.
[7] P. Schmid and P. Huber, Helv. Phys. Acta 27 (1954) 152.
[8] L.C. Henry and T.J. Kennett, Can. J. Phys. 50 (1972) 2756.

North-Holland Publishing Company, P.O. Box 103, Amsterdam
Northprint: 13E
Page: 5 1st proof:
IN ALL CORRESPONDENCE CONCERNING THIS PAPER REFER TO:
NIM101844

7 APR. 1983

Nuclear Instruments and Methods 0 (1983) NIM01844 [NC]
North-Holland Publishing Company

A METHOD OF STUDYING ATOMIC SCREENING EFFECTS IN PAIR PRODUCTION

Jahnabi BOSE, Nanak BHATTACHARJEE, Swapan Kumar SENGUPTA * and N. CHAUDHURI
Department of Physics, North Bengal University, Raja Rammohunpur, Darjeeling, India 734430

Received 6 September 1982

A simple method to study atomic screening effects in atomic pair production has been used in measurements using 1.115 MeV photons on medium and high Z targets in the range of atomic number 29–92. Some of the results are presented and discussed.

1. Introduction

In a previous paper [1] the development of a simple method for studying atomic screening effects in pair production was reported. This method has been applied in a continuing series of measurements using photons of energy near threshold for studying screening effects in atomic pair production. The method has the following advantages:

1) Separate measurements of the annihilation pair production detection efficiency is not needed in the evaluation of a cross section relative to a standard cross section.
2) The total gamma-ray absorption coefficients of the target material do not enter into the computation of the cross section.
3) A large number of corrections to the data is avoided.
4) A resolution time of 40 ns has been achieved by improved electronics.
5) The continuum background does not affect the result and there is no problem in the analysis of the very well defined simple pair annihilation peak obtained by a NaI(Tl) detector.
6) The method is suitable for testing new theoretical screening corrections to the pair production cross section.

The present paper reports new results of measurements by this method using photons of energy 1.115 MeV from a 100 mCi radioactive source ^{65}Zn.

2. Experimental procedure

The experimental arrangement is shown in fig. 1. Details of the method have already been described [1]. Only essential points relevant to the present paper are given here. The measuring system includes a coincidence stage having a resolving time of about 40 ns. The output resulting from coincidence between the two detectors was used to gate a multichannel analyser (M) which recorded the 0.511 MeV annihilation spectra from one of the detectors. The gamma-ray source was in the form of a cylindrical pellet placed in a 30 cm deep and 1.8 cm diameter bored lead block. The radiators of copper, tin, gold, thorium and uranium were in the form of circular targets of diameter 2 cm and thickness in the range 0.012–0.62 g/cm^2. The targets were thin for the incident gamma-rays but thick enough to stop the positrons of the produced pair.

The intensity of the annihilation quanta determined from the area of the photopeak of the sample target "X" of atomic number Z was compared with that of a similar lower Z comparison radiator (taken as standard) both taken in exactly the same geometry. The standard radiator element chosen was copper ($Z = 29$) because this gives counts of annihilation quanta of better statistics and the effect of trident production and incoherent pair production is negligibly small at such an intermediate atomic number. This procedure gives for the cross section ratio

$$\frac{\sigma_X}{\sigma_{Cu}} = \frac{C_X A_X}{C_{Cu} A_{Cu}}, \qquad (1)$$

where C and A are, respectively, the intensity of annihilation quanta per gcm^{-2} and the atomic weight. Suffixes X and Cu refer to target element X and standard radiator copper.

An improvement in the measurements of two-photon annihilation events, 180° apart, has been achieved by eliminating effects due to (1) absorption of annihilation quanta in the target, (2) absorption of incident photons in the target, (3) background (chance and false coincidences) resulting from interactions other than pair production in the target and background materials, and (4)

* University Service and Instrumentation Centre (USIC), North Bengal University, Darjeeling-734430, India.

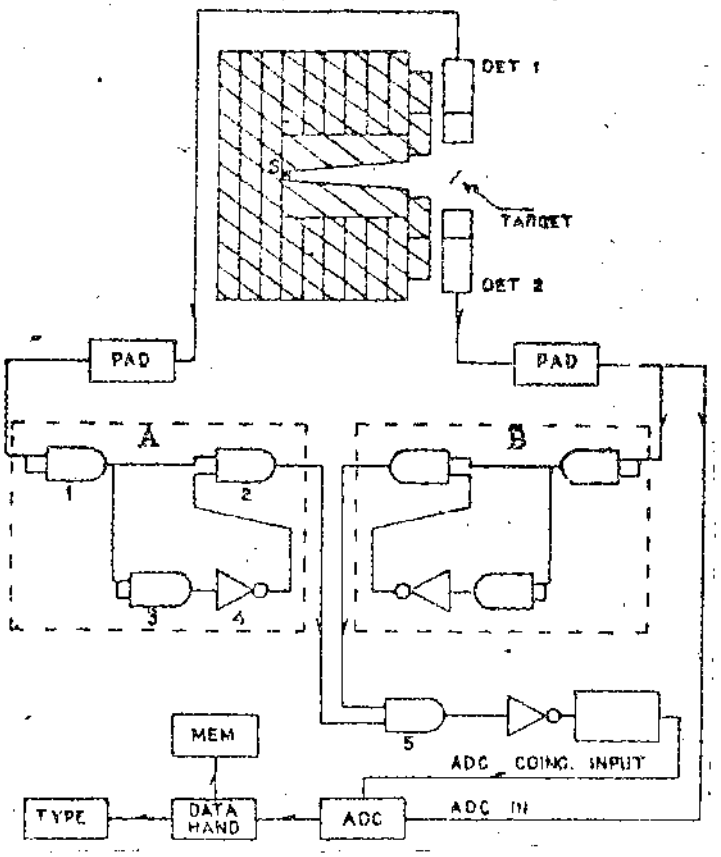

Fig. 1. Experimental arrangement showing source–target–detector geometry along with the block diagram of the associated electronics.

the effect of short term variation of the detection efficiency of annihilation photon.

The corrections arising from the effects (1) and (2) have been eliminated by measuring the coincidence rate from varying thicknesses of the targets. To minimize the effects (3) and (4), the data were taken alternately on each set of standard and sample targets in the following sequence: standard target (coincidence rate at 180° and at 90° between the axes of the two detectors), sample targets (coincidence rate at 180° and 90° positions of the two detectors), background coincidences at the two positions with and without target, standard target, and so on. The counting time for the sequence was adjusted to obtain a satisfactory statistical error level. The shapes of the background spectra without target at 180° and 90° positions are found to be exactly identical. The samples and "standard" coincidence rates at 90° position have been taken as the chance coincidence rate in the determination of the pair annihilation coincidence rate at 180° position and has been used to correct the observed coincidence spectrum. A selection of background and observed annihilation spectra at 180° is shown in fig. 2. The true coincidence rates (N), for various thicknesses of each element, of the positron electron pair thus determined were found to fit the expression

$$N = Ct\,e^{-at}, \qquad (2)$$

where t is the target thickness in gcm^{-2} and C is the true two-photon coincidence count rate for a target of thickness 1 gcm^{-2} and a is a constant for a given element. The constants C and a were determined through the proper fitting procedure. The obtained fit to the data for five elements is shown in fig. 3.

The present measurements are free from some of the possible systematic errors because the ratio of two annihilation radiation peak counts in identical geometry has been taken.

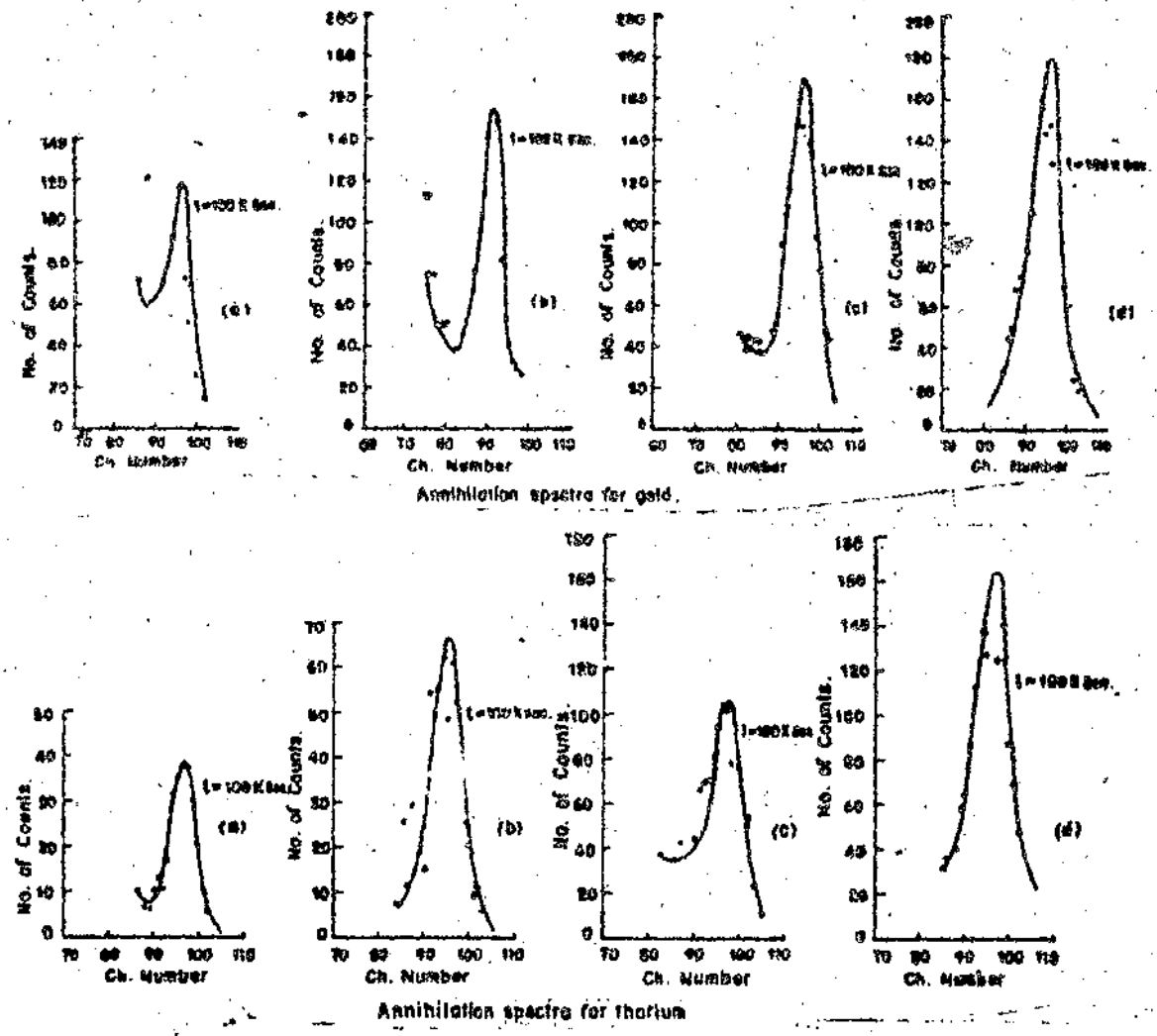

Fig. 2. Observed annihilation spectra for gold (*upper*) and thorium (*lower*) at 180° position showing observed *counts* (dots) fitted curve (*full* line); (a), (b), (c), and (d) give the above spectra of increased thickness.

Table 1
Theoretical and experimental pair production cross section ratios.

Ratio	Theoretical [a]				Experimental
	Born approximation	Øverbø [2] PC	Øverbø SC	Tseng Pratt [3] SC	
σ_{Sn}/σ_{Cu}	2.970	3.335	3.587	3.640	3.770 ± 0.2
σ_{Au}/σ_{Cu}	7.40	6.380	10.580	8.990	10.530 ± 0.7
σ_{Th}/σ_{Cu}	9.620	6.810	14.410	11.007	12.400 ± 0.9
σ_{U}/σ_{Cu}	10.062	6.830	15.660	11.380	13.180 ± 0.9

[a] PC – point Coulomb approximation cross section ratio. SC – screening corrected cross section ratio.

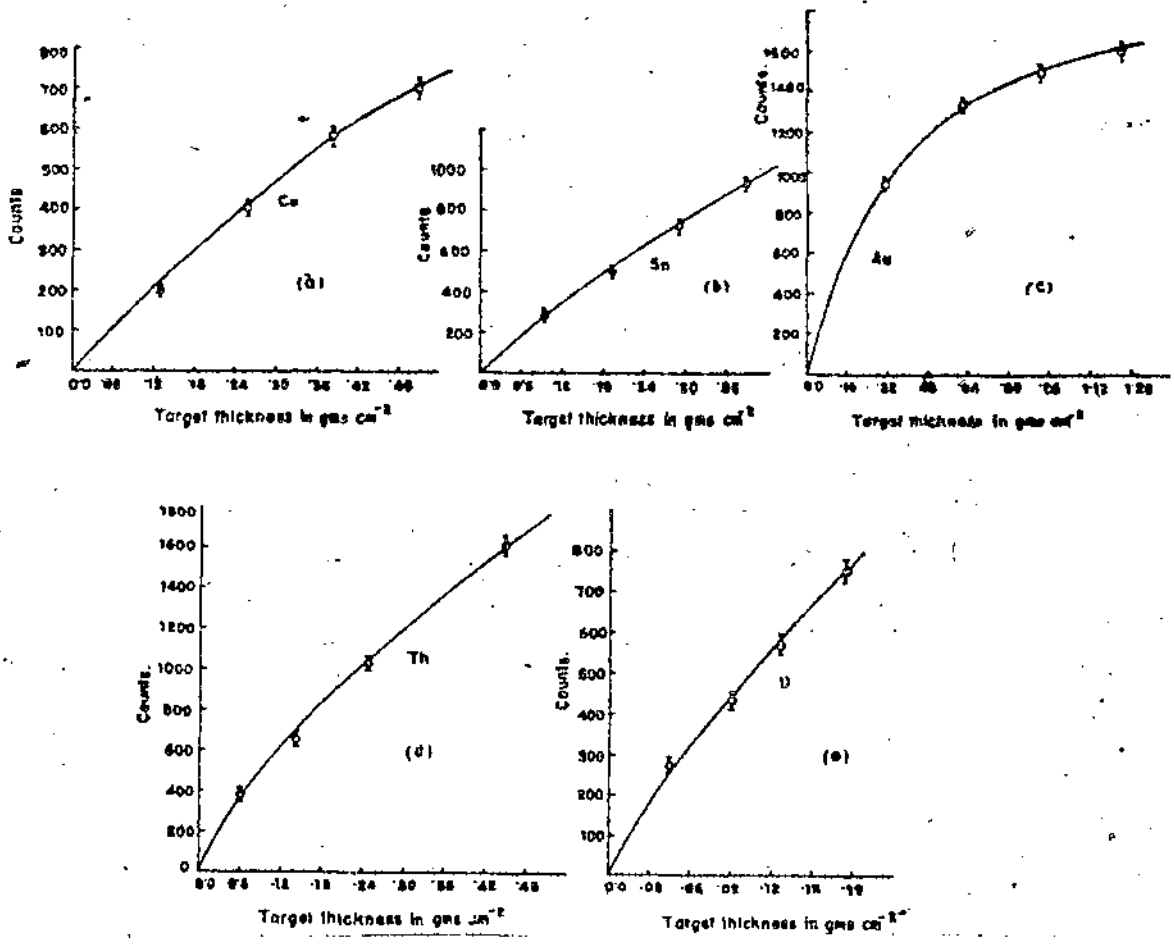

Fig. 3. Observed total counts (dots) plotted against target thickness (gcm^{-2}); full line: fitted curve according to eq. (2); (a), (b), (c), (d), and (e) for copper, tin, gold, thorium and uranium respectively.

3. Results and discussion

The results for cross section ratios from our measurements together with those obtained from some recent theoretical predictions are given in table 1. The theoretical cross section for the standard element (copper) for 1.115 MeV gamma-rays is 9.64×10^{-4} b/atom according to Øverbø [2] and 9.63×10^{-4} b/atom according to

Table 2
Theoretical and experimental pair production cross section (b $atom^{-1}$) at 1.115 MeV.

Element	Born approximation	Øverbø [a] [2] PC	Øverbø [a] [2] SC	Tseng [a] [3] Pratt SC	Present experimental, taking the cross section value of copper as:	
					9.64×10^{-4} from ref. 2.	9.63×10^{-4} from ref. 3.
Sn	1.895×10^{-3}	3.017×10^{-3}	3.460×10^{-3}	3.520×10^{-3}	$(3.634 \pm 0.019) 10^{-3}$	$(3.630 \pm 0.019) 10^{-3}$
Au	4.733×10^{-3}	5.774×10^{-3}	1.02×10^{-2}	8.660×10^{-3}	0.0101 ± 0.006	0.0101 ± 0.006
Th	6.142×10^{-3}	6.160×10^{-3}	1.390×10^{-2}	1.060×10^{-2}	0.0119 ± 0.008	0.0119 ± 0.008
U	6.418×10^{-3}	6.184×10^{-3}	1.510×10^{-2}	1.096×10^{-2}	0.0127 ± 0.008	0.0126 ± 0.008

[a] PC – point Coulomb approximation cross section; SC – screening corrected cross section.

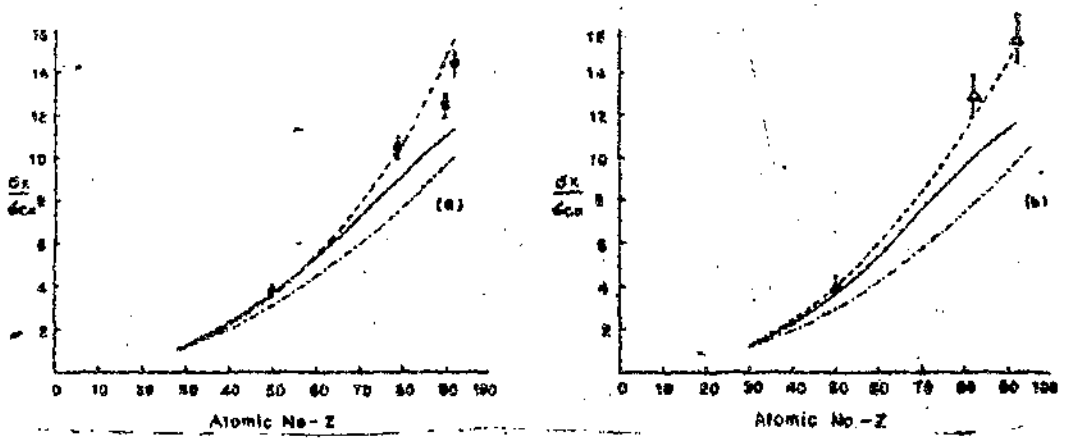

Fig. 4. Graphs showing $(\sigma_x/\sigma_{C_{Pb}})_{0,Z}$ according to Born approximations (dash–dot line) according to screening corrections, of Øverbø [2] (dashed line) according to Tseng and Pratt [3] (full line) at (a) 1.115 MeV, (b) 1.119 MeV. Experimental points: circles present experiment, triangles Girard et al. [4].

Tseng and Pratt [3]. Taking these values with our experimental results of cross section ratios of table 1, the extracted experimental values for tin, gold, thorium and uranium are given in table 2. As shown in fig. 4, it is easier to check experimentally the screening correction in the presently adopted method which is independent of various sources of errors and which were found to be very difficult to avoid in earlier direct experiments [4].

The effect of screening on the cross section of pair production near threshold is important for atoms of larger atomic number. The results presented in this paper demonstrate the suitability of the present method in making a direct check on the screening correction on pair production in high Z atoms at energies very near threshold.

The authors are grateful to the University of North Bengal for providing a U.G.C. Teacher Fellowship to *J. Basu* and *N. Bhattacharjee*.

References

[1] J. Bose et al., Nucl. Instr. and Meth. 200 (1982) 265.
[2] I. Øverbø, Phys. Scr. 19 (1979) 299, Thesis work (1967) (unpublished).
[3] H.K. Tseng and R.H. Pratt, Phys. Rev. A 6 (1972) 2049.
[4] T.A. Girard, F.T. Avignone III and S.M. Blankenship, Phys. Rev. A 17 (1978) 218, Phys. Lett. 71A (1979) 33.